

Prepared in cooperation with the Federal Emergency Management Agency

Characterization of Peak Streamflows and Flood Inundation of Selected Areas in Southeastern Texas and Southwestern Louisiana from the August and September 2017 Flood Resulting from Hurricane Harvey



Scientific Investigations Report 2018–5070

Front cover, Photograph showing the area where Townsen Boulevard intersects U.S. Highway 59, about 0.65 mile southwest of USGS streamflow-gaging station 08069500, West Fork San Jacinto River near Humble, Texas, August 30, 2017. Perspective of the photo is looking downstream, and the right flood plain of the West Fork San Jacinto River is shown. Photograph courtesy of Steve Fitzgerald, Harris County Flood Control District, used with permission.

Back cover:

Upper left, Photograph showing Addicks Reservoir looking upstream from top of dam with outlet works and lake station (USGS 08073000, Addicks Reservoir near Addicks, TX), August 29, 2017. Addicks Reservoir is a flood-control reservoir for the City of Houston, and its spillway is located about 12 miles north of Sugar Land, Texas. Photograph by Robert Ellis, Hydrologic Technician with the U.S. Geological Survey Gulf Coast Texas Program Office in Houston, Texas.

Upper right, Photograph showing Addicks Reservoir looking upstream from top of dam with outlet works and lake station (USGS 08073000, Addicks Reservoir near Addicks, TX), April 6, 2018. Addicks Reservoir is a flood-control reservoir for the City of Houston, and its spillway is located about 12 miles north of Sugar Land, Texas. Photograph by Tom Pistillo, Hydrologic Technician with the U.S. Geological Survey Gulf Coast Texas Program Office in Houston, Texas.

Lower left, Photograph showing Brandon Cooper, Hydrologic Technician with the U.S. Geological Survey, flagging a debris line on a telephone pole approximately 14.3 feet above the ground and located about 245 feet east of the bridge on Keith Road over Boggy Creek, September 15, 2017. Photograph by Melissa Null, Hydrologist with the U.S. Geological Survey North Texas Program Office in Fort Worth, Texas.

Lower right, Photograph showing U.S. Geological Survey streamflow-gaging station 08072600, Buffalo Bayou at State Highway 6 near Addicks, Texas, looking south on State Highway 6, August 31, 2017. The streamflow-gaging station is located about 10.5 miles north of Sugar Land, Texas. Barker Reservoir, a flood-control reservoir for the City of Houston, is to the right in the photo, and streamflow consists of releases from the reservoir. Photograph by MacKenzie Mullins, Hydrologic Technician with the U.S. Geological Survey Gulf Coast Texas Program Office in Houston, Texas.

Characterization of Peak Streamflows and Flood Inundation of Selected Areas in Southeastern Texas and Southwestern Louisiana from the August and September 2017 Flood Resulting from Hurricane Harvey

By Kara M. Watson, Glenn R. Harwell, David S. Wallace, Toby L. Welborn,
Victoria G. Stengel, and Jeremy S. McDowell

Prepared in cooperation with the Federal Emergency Management Agency

Scientific Investigations Report 2018–5070

**U.S. Department of the Interior
U.S. Geological Survey**

U.S. Department of the Interior
RYAN K. ZINKE, Secretary

U.S. Geological Survey
James F. Reilly II, Director

U.S. Geological Survey, Reston, Virginia: 2018

For more information on the USGS—the Federal source for science about the Earth, its natural and living resources, natural hazards, and the environment—visit <https://www.usgs.gov> or call 1–888–ASK–USGS.

For an overview of USGS information products, including maps, imagery, and publications, visit <https://www.usgs.gov/pubprod/>.

Inundated areas shown should not be used for navigation, regulatory, permitting, or other legal purposes. The U.S. Geological Survey provides these maps “as-is” for a quick reference, emergency planning tool but assumes no legal liability or responsibility resulting from the use of this information.

Any use of trade, firm, or product names is for descriptive purposes only and does not imply endorsement by the U.S. Government.

Although this information product, for the most part, is in the public domain, it also may contain copyrighted materials as noted in the text. Permission to reproduce copyrighted items must be secured from the copyright owner.

Suggested citation:

Watson, K.M., Harwell, G.R., Wallace, D.S., Welborn, T.L., Stengel, V.G., and McDowell, J.S., 2018, Characterization of peak streamflows and flood inundation of selected areas in southeastern Texas and southwestern Louisiana from the August and September 2017 flood resulting from Hurricane Harvey: U.S. Geological Survey Scientific Investigations Report 2018–5070, 44 p., <https://doi.org/10.3133/sir20185070>.

ISSN 2328-0328 (online)

Acknowledgments

The authors would like to thank the staff of the Texas Natural Resources Information System, the Federal Emergency Management Agency, and the U.S. Geological Survey (USGS) who provided the digital elevation data necessary to complete this assessment. A special thanks is extended to Claire DeVaughan, USGS National Map Liaison for Texas and Oklahoma, for identifying data resources and interagency contacts to acquire these data.

Contents

Acknowledgments	iii
Abstract	1
Introduction	1
Purpose and Scope	7
Description of Study Area	7
Weather Conditions Before and During the Flood	7
Methods	8
Collection of High-Water Mark Data	8
Flood-Inundation Mapping	11
Flood Exceedance Probabilities of Peak Streamflows	11
Estimated Magnitudes and Flood Exceedance Probabilities of Peak Streamflows	16
Flood-Inundation Maps	16
Brazos River and Tributaries	16
Neches River and Tributaries	19
Pine Island Bayou	19
Sabine River and Tributaries	23
Big Cow Creek	27
Cow Bayou	27
San Bernard River	27
San Jacinto River and Tributaries	33
Coastal Basins	37
East Matagorda Bay Subbasin	37
Peak Water-Surface Elevations for Coastal Areas	42
Flood Damages	42
Summary	42
References Cited	42

Figures

1. Map showing rainfall totals in southeastern Texas and southwestern Louisiana from August 25 through September 1, 2017, resulting from Hurricane Harvey and locations of physiographic sections and climate divisions	2
2. Map showing the locations of U.S. Geological Survey streamflow-gaging stations used to calculate annual exceedance probabilities and rainfall totals from August 25 through September 1, 2017, resulting from Hurricane Harvey	4
3. Map showing locations of U.S. Geological Survey streamflow-gaging stations, selected cities and counties, parishes, and river basins within the study area in southeastern Texas and southwestern Louisiana	12
4. Flood-inundation map of the upper reach of the Brazos River for the August and September 2017 Hurricane Harvey-related flood event in southeastern Texas and southwestern Louisiana	17
5. Flood-inundation map of the lower reach of the Brazos River for the August and September 2017 Hurricane Harvey-related flood event in southeastern Texas and southwestern Louisiana	18

6.	Flood-inundation map of the upper reach of the Neches River for the August and September 2017 Hurricane Harvey-related flood event in southeastern Texas and southwestern Louisiana	20
7.	Flood-inundation map of the lower reach of the Neches River for the August and September 2017 Hurricane Harvey-related flood event in southeastern Texas and southwestern Louisiana	21
8.	Flood-inundation map of Pine Island Bayou, a tributary to the Neches River, for the August and September 2017 Hurricane Harvey-related flood event in southeastern Texas and southwestern Louisiana	22
9.	Flood-inundation map of the upper reach of the Sabine River for the August and September 2017 Hurricane Harvey-related flood event in southeastern Texas and southwestern Louisiana	24
10.	Flood-inundation map of the middle reach of the Sabine River for the August and September 2017 Hurricane Harvey-related flood event in southeastern Texas and southwestern Louisiana	25
11.	Flood-inundation map of the lower reach of the Sabine River for the August and September 2017 Hurricane Harvey-related flood event in southeastern Texas and southwestern Louisiana	26
12.	Flood-inundation map of Big Cow Creek, a tributary to the Sabine River, for the August and September 2017 Hurricane Harvey-related flood event in southeastern Texas and southwestern Louisiana	28
13.	Flood-inundation map of Cow Bayou, a tributary to the Sabine River, for the August and September 2017 Hurricane Harvey-related flood event in southeastern Texas and southwestern Louisiana	29
14.	Flood-inundation map of the upper reach of the San Bernard River for the August and September 2017 Hurricane Harvey-related flood event in southeastern Texas and southwestern Louisiana	30
15.	Flood-inundation map of the middle reach of the San Bernard River for the August and September 2017 Hurricane Harvey-related flood event in southeastern Texas and southwestern Louisiana	31
16.	Flood-inundation map of the lower reach of the San Bernard River for the August and September 2017 Hurricane Harvey-related flood event in southeastern Texas and southwestern Louisiana	32
17.	Flood-inundation map of the West Fork San Jacinto River and its tributaries for the August and September 2017 Hurricane Harvey-related flood event in southeastern Texas and southwestern Louisiana	35
18.	Flood-inundation map of the East Fork San Jacinto River and its tributaries for the August and September 2017 Hurricane Harvey-related flood event in southeastern Texas and southwestern Louisiana	36
19.	Flood-inundation map of Peyton Creek, Big Boggy Creek, and Little Boggy Creek for the August and September 2017 Hurricane Harvey-related flood event in southeastern Texas and southwestern Louisiana	38
20.	Flood-inundation map of the Tres Palacios River for the August and September 2017 Hurricane Harvey-related flood event in southeastern Texas and southwestern Louisiana	39
21.	Flood-inundation map of the East and West Carancahua Creeks and the Keller Creek for the August and September 2017 Hurricane Harvey-related flood event in southeastern Texas and southwestern Louisiana	40
22.	Flood-inundation map from coastal water-surface elevation data for the August and September 2017 Hurricane Harvey-related flood event in southeastern Texas and southwestern Louisiana	41

Tables

1. Rainfall totals resulting from Hurricane Harvey reported at 38 National Oceanic and Atmospheric Administration meteorological stations and 2 Jefferson County Drainage District rain gages in southeastern Texas from August 25 through September 1, 20173
2. U.S. Geological Survey streamflow-gaging stations in southeast Texas with at least 15 years of record, no large data gaps in the period of record, and a 2017 annual peak streamflow ranking in the top five of all annual peaks for a given station that were used to calculate annual exceedance probabilities5
3. Peak gage heights, peak streamflows, and estimated annual exceedance probabilities for the August and September 2017 Hurricane Harvey-related flood event at 74 selected U.S. Geological Survey streamflow-gaging stations in southeastern Texas9
4. Counties, parishes, waterbodies, reach lengths, and number of high-water marks used to generate flood-inundation maps13
5. Site identification number, station number, and expected peak streamflows for selected annual exceedance probabilities with 95 percent confidence intervals at 74 selected U.S. Geological Survey streamflow-gaging stations in southeastern Texas14

Conversion Factors

U.S. customary units to International System of Units

Multiply	By	To obtain
Length		
inch (in.)	2.54	centimeter (cm)
inch (in.)	25.4	millimeter (mm)
foot (ft)	0.3048	meter (m)
mile (mi)	1.609	kilometer (km)
Area		
square mile (mi ²)	259.0	hectare (ha)
square mile (mi ²)	2.590	square kilometer (km ²)
Flow rate		
cubic foot per second (ft ³ /s)	0.02832	cubic meter per second (m ³ /s)
mile per hour (mi/h)	1.609	kilometer per hour (km/h)

Datum

Vertical coordinate information is referenced to the North American Vertical Datum of 1988 (NAVD 88) and the National Geodetic Vertical Datum of 1929 (NGVD 29).

Horizontal coordinate information is referenced to the North American Datum of 1983 (NAD 83).

Elevation as used in this report, refers to distance above the vertical datum.

Abbreviations

AEP	annual exceedance probability
DEM	digital elevation model
FEMA	Federal Emergency Management Agency
GIS	geographic information system
GPS	Global Positioning System
HWM	High-water mark
Lidar	light detection and ranging
NOAA	National Oceanic and Atmospheric Administration
NWS	National Weather Service
STN	Short-Term Network (USGS)
USGS	U.S. Geological Survey

Characterization of Peak Streamflows and Flood Inundation of Selected Areas in Southeastern Texas and Southwestern Louisiana from the August and September 2017 Flood Resulting from Hurricane Harvey

By Kara M. Watson, Glenn R. Harwell, David S. Wallace, Toby L. Welborn, Victoria G. Stengel, and Jeremy S. McDowell

Abstract

Hurricane Harvey made landfall near Rockport, Texas, on August 25, 2017, as a Category 4 hurricane with wind gusts exceeding 150 miles per hour. As Harvey moved inland, the forward motion of the storm slowed down and produced tremendous rainfall amounts over southeastern Texas, with 8-day rainfall amounts exceeding 60 inches in some locations, which is about 15 inches more than average annual amounts of rainfall for eastern Texas and the Texas coast. Historic flooding occurred in Texas as a result of the widespread, heavy rainfall; wind and flood damages were estimated to be \$125 billion, and the storm resulted in at least 68 direct fatalities.

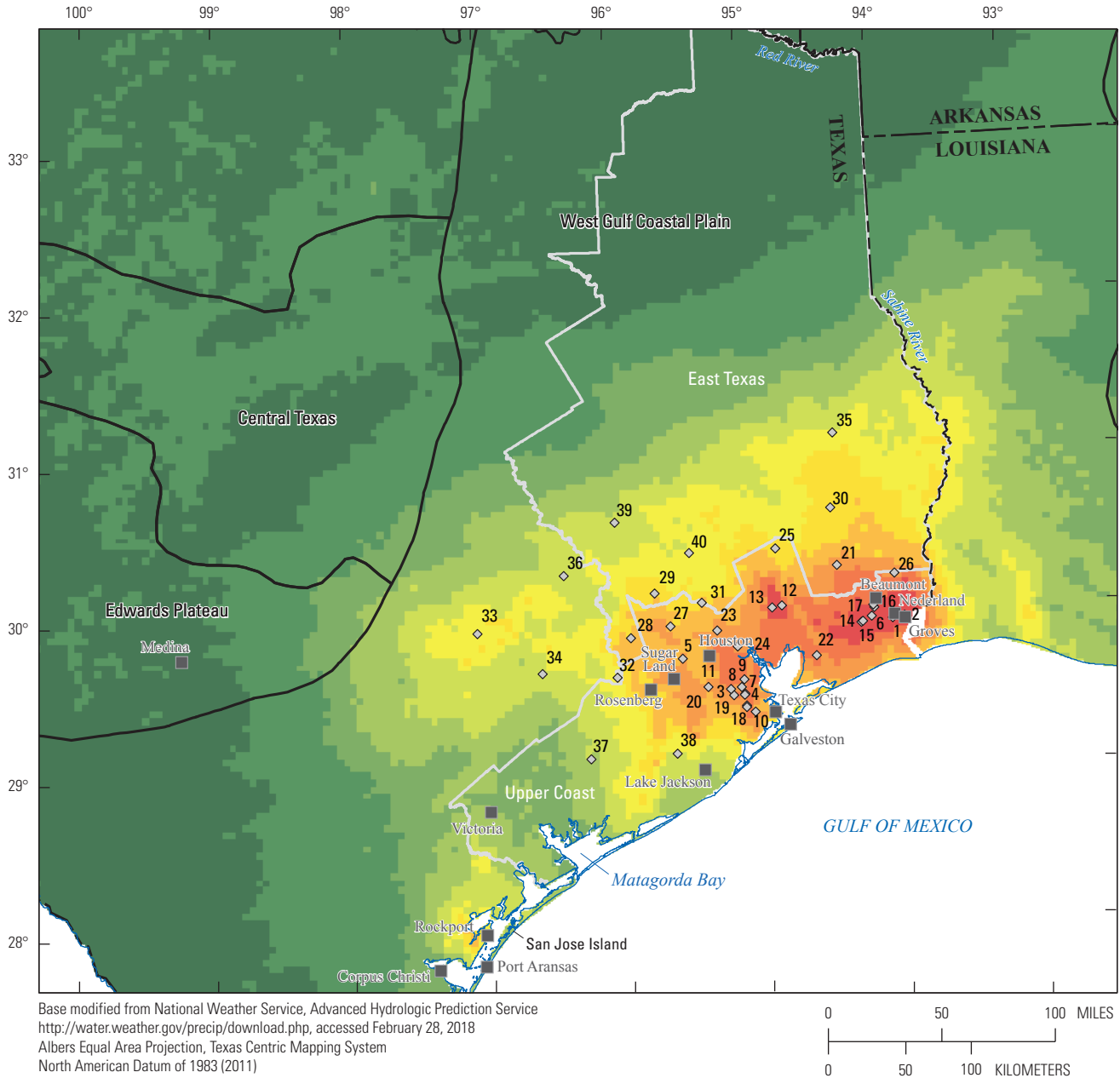
In the immediate aftermath of the Harvey-related flood event, the U.S. Geological Survey (USGS) and the Federal Emergency Management Agency initiated a cooperative study to evaluate the magnitude of the flood, determine the probability of occurrence, and map the extent of the flood in Texas. Seventy-four USGS streamflow-gaging stations in Texas with at least 15 years of record and no large data gaps in the period of record had a 2017 annual peak streamflow related to Harvey ranking in the top five of all annual peaks for each given station. New peaks of record streamflow were recorded at 40 of the 74 USGS streamflow-gaging stations. The number of years of peak streamflow record for the 74 analyzed streamflow-gaging stations ranged from 18 to 105, with a mean number of 55 years. The annual exceedance probability estimates for the analyzed streamflow-gaging stations ranged from less than 0.2 to 14.0 percent. USGS field crews surveyed 2,123 high-water marks to obtain water-surface elevations, in feet above the North American Vertical Datum of 1988. In some locations, several water-surface elevations were averaged to obtain 1 water-surface elevation, resulting in 1,258 water-surface elevations. Some of these high-water marks were used, along with peak-stage data from

USGS streamflow-gaging stations, to create 19 inundation maps to document the areal extent of the maximum depth of the flooding. Digital datasets of the inundation area, modeling boundary, water-depth rasters, and final map products are available from the USGS data release associated with this report (<https://doi.org/10.5066/F7VH5N3N>).

Introduction

On August 17, 2017, Hurricane Harvey (referred to hereinafter as Harvey) entered the Caribbean Sea as a tropical storm, but it became disorganized and was downgraded to a tropical wave as it entered the Gulf of Mexico on August 22 (National Oceanic and Atmospheric Administration [NOAA], 2018a). During the next 72 hours, however, Harvey intensified into a Category 4 hurricane and made landfall near Rockport, Texas, about 10:00 p.m. on August 25 with wind gusts exceeding 150 miles per hour (mi/h) (NOAA, 2018b). As Harvey moved inland, the forward motion of the storm slowed down and produced tremendous rainfall amounts in southeastern Texas and southwestern Louisiana, with 8-day rainfall amounts exceeding 60 inches (in.) in some areas of Texas (Blake and Zelinsky, 2018; fig. 1; table 1). Historic flooding accompanied by extensive wind damage occurred in Texas and Louisiana as a result of the widespread, heavy rainfall (NOAA, 2018c). In the immediate aftermath of the Harvey-related flood event, the U.S. Geological Survey (USGS) and the Federal Emergency Management Agency (FEMA) initiated a cooperative study to evaluate the magnitude of the flood, determine the probability of occurrence, and map the extent of the flood in selected river basins in Texas. For this study, flood-peak streamflow data that were recorded at 74 streamflow-gaging stations operated by the USGS in southeastern Texas were selected for analysis (fig. 2; table 2).

2 Characterization of Peak Streamflows and Flood Inundations from Hurricane Harvey, 2017



EXPLANATION

Rainfall totals, in inches, from August 25 through September 1, 2017

- 0 to 1
- 1.1 to 5
- 5.1 to 10
- 10.1 to 15
- 15.1 to 20
- 20.1 to 25
- 25.1 to 30
- 30.1 to 35
- 35.1 to 40
- 40.1 to 45

— Contiguous United States (CONUS) Climate Divisions, from National Oceanic and Atmospheric Administration (2017)

— Physiographic section boundary, from Fenneman (1946)

◆ National Oceanic and Atmospheric Administration meteorological station and site identification number—Station number listed in table 1

Note: The record rainfall amounts of 60.58 and 60.54 inches listed in table 1 are from Jefferson County Drainage District rain gages, which were probably not used by the National Weather Service to create the maps depicting rainfall amounts in the study area; to create maps of rainfall amounts, the National Weather Service averages rainfall over large areas, which could also account for discrepancies between the maximum rainfall amounts depicted in figs. 1–2 and individual point values exceeding 60 inches of rain listed in table 1.

Figure 1. Rainfall totals in southeastern Texas and southwestern Louisiana from August 25 through September 1, 2017, resulting from Hurricane Harvey and locations of physiographic sections and climate divisions.

Table 1. Rainfall totals resulting from Hurricane Harvey reported at 38 National Oceanic and Atmospheric Administration meteorological stations and 2 Jefferson County Drainage District rain gages in southeastern Texas from August 25 through September 1, 2017 (Blake and Zelinsky, 2018).

[N, north; S, south; E, east; W, west; I, Interstate]

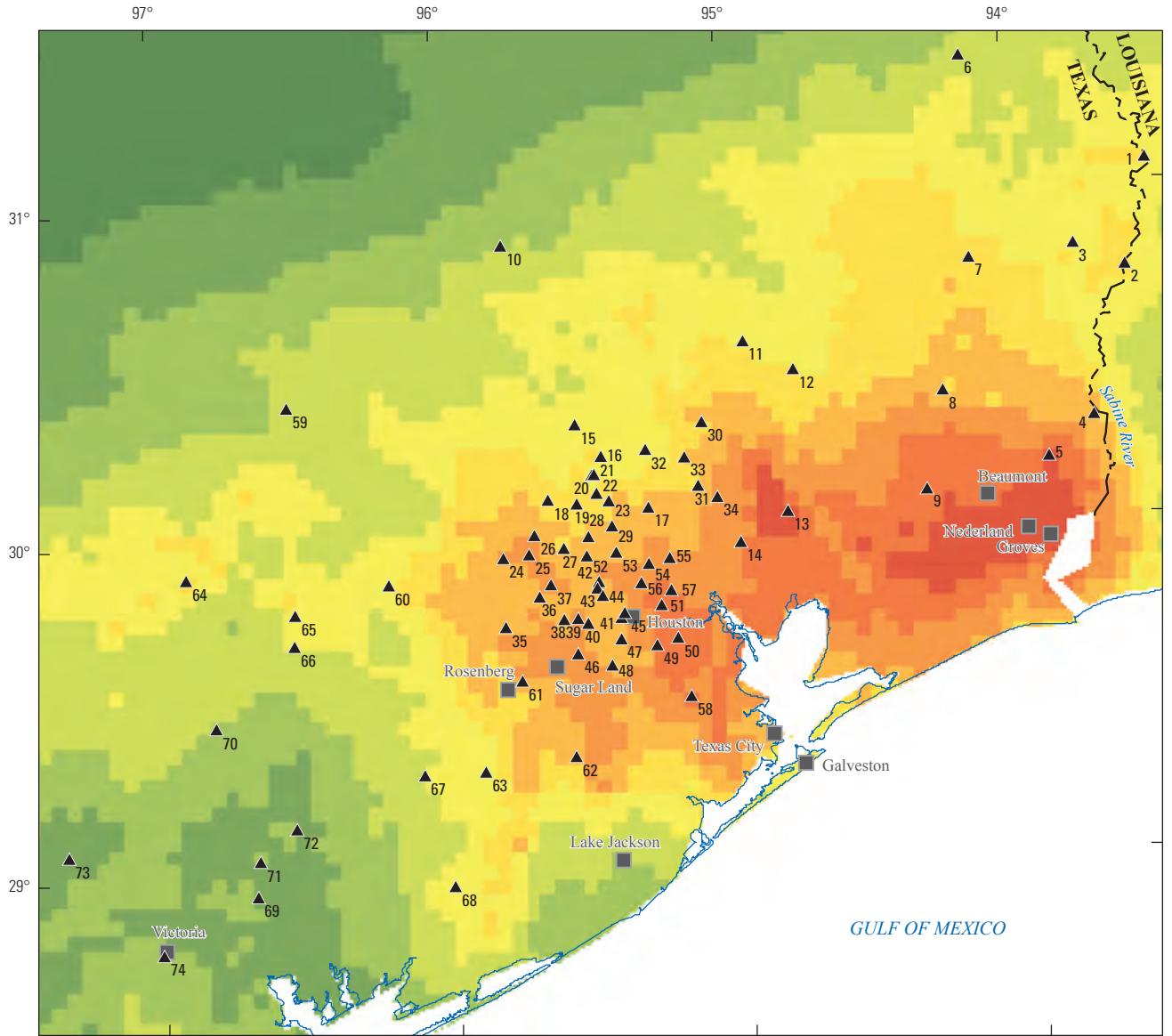
Site identification number (fig. 1)	Station name ¹	County	Latitude (decimal degrees)	Longitude (decimal degrees)	Rainfall total (inches) ²
³ 1	Nederland 1.5 SW	Jefferson	29.95	94.01	60.58
³ 2	Groves 1.3 N	Jefferson	29.96	93.92	60.54
3	Friendswood	Galveston	29.50	95.20	56.00
4	Santa Fe 3 ENE	Galveston	29.39	95.05	54.77
5	Friendswood	Harris	29.75	95.57	54.00
6	Labelle Road Pevito Bayou	Jefferson	29.96	94.17	53.82
7	League City 3 S	Galveston	29.43	95.11	52.87
8	Webster 2 NW	Harris	29.55	95.14	52.30
9	Ellington Field 2 E	Harris	29.60	95.12	52.00
10	League City 4 S	Galveston	29.42	95.11	51.62
11	Friendswood 2 NNW	Brazoria	29.54	95.22	50.04
12	Liberty 2 WSW	Liberty	30.06	94.82	49.39
13	Dayton 0.2 E	Liberty	30.05	94.89	49.31
14	Fannett 1 NE	Jefferson	29.93	94.24	49.25
15	Glenbrook Drive at Green Acres at Ditch 407	Jefferson	29.94	94.23	49.25
16	Beaumont 4 S	Jefferson	30.02	94.14	49.06
17	State Highway 124 at Hillebrandt Bayou	Jefferson	30.04	94.15	49.06
18	Clear Creek at I-45	Harris	29.51	95.12	48.20
19	Webster 2 S	Galveston	29.50	95.12	48.20
20	Clear Lake	Brazoria	29.56	95.39	48.14
21	Pine Ridge 4 NNW	Hardin	30.30	94.40	42.60
22	East Fork of DB at Fairview Road	Chambers	29.73	94.58	41.57
23	Greens Bayou at US 59	Harris	29.92	95.31	37.60
24	Carpenters Bayou at Wallisville Road	Harris	29.81	95.16	37.44
25	Romayor/Trinity River	Liberty	30.43	94.85	30.10
26	Vidor 7.2 N	Orange	30.23	93.98	29.64
27	Cypress 3.2 ESE	Harris	29.96	95.65	27.83
28	Brookshire Katy Drainage District at Morrison Road	Waller	29.89	95.94	27.04
29	Magnolia 2.8 S	Montgomery	30.17	95.76	26.93
30	Woodville 7.2 S	Tyler	30.67	94.43	25.01
31	Pinehurst 0.4 SSE	Montgomery	30.10	95.41	23.85
32	Wallis 1.1 NE	Austin	29.64	96.05	21.83
33	Smithville 6.6 SE	Fayette	29.95	97.07	21.72
34	Columbus 3.2 WSW	Colorado	29.68	96.60	21.39
35	Zavalla 2.0 ESE	Angelina	31.15	94.39	20.27
36	Brenham 9.9 N	Washington	30.30	96.42	18.80
37	El Campo 4.9 SSE	Wharton	29.13	96.26	15.16
38	West Columbia 1 ESE	Brazoria	29.14	95.63	10.16
39	Carlos 3 NE	Grimes	30.63	96.03	6.04
40	Willis 1 SW	Montgomery	30.42	95.49	5.00

¹Station name taken directly from https://www.nhc.noaa.gov/data/tcr/AL092017_Harvey.pdf (Blake and Zelinsky, 2018).

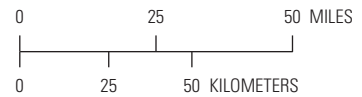
²Rainfall total from August 25 through September 1, 2017.

³Jefferson County Drainage District rain gage.

4 Characterization of Peak Streamflows and Flood Inundations from Hurricane Harvey, 2017

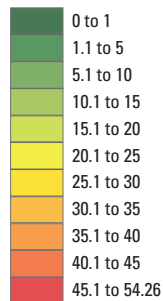


Base modified from National Weather Service, Advanced Hydrologic Prediction Service 1:1,000,000 scale digital data <http://water.weather.gov/precip/download.php>, accessed February 28, 2018
 Albers Equal Area Projection, Texas Centric Mapping System
 North American Datum of 1983 (2011)



EXPLANATION

Rainfall totals, in inches, from August 25 through September 1, 2017



▲ U.S. Geological Survey streamflow-gaging station used to calculate annual exceedance probabilities and associated site identification number—Station number listed in table 2

Note: The record rainfall amounts of 60.58 and 60.54 inches listed in table 1 are from Jefferson County Drainage District rain gages, which were probably not used by the National Weather Service to create the maps depicting rainfall amounts in the study area; to create maps of rainfall amounts, the National Weather Service averages rainfall over large areas, which could also account for discrepancies between the maximum rainfall amounts depicted in figs. 1–2 and individual point values exceeding 60 inches of rain listed in table 1.

Figure 2. The locations of U.S. Geological Survey streamflow-gaging stations used to calculate annual exceedance probabilities and rainfall totals from August 25 through September 1, 2017, resulting from Hurricane Harvey.

Table 2. U.S. Geological Survey streamflow-gaging stations in southeast Texas with at least 15 years of record, no large data gaps in the period of record, and a 2017 annual peak streamflow ranking in the top five of all annual peaks for a given station that were used to calculate annual exceedance probabilities.

[mi², square miles]

Site identification number (fig. 2)	Station number	Station name	Drainage area (mi ²)	Latitude (decimal degrees)	Longitude (decimal degrees)
1	08026000	Sabine River near Burkeville, Texas	7,482	31.06408	93.51962
2	08028500	Sabine River near Bon Wier, Texas	8,229	30.74715	93.60851
3	08029500	Big Cow Creek near Newton, Texas	128	30.81889	93.78556
4	08030500	Sabine River near Ruliff, Texas	9,329	30.30382	93.74378
5	08031000	Cow Bayou near Mauriceville, Texas	83.3	30.18632	93.90851
6	08039100	Ayish Bayou near San Augustine, Texas	89.0	31.39630	94.15103
7	08040600	Neches River near Town Bluff, Texas	7,574	30.79104	94.15102
8	08041500	Village Creek near Kountze, Texas	860	30.39799	94.26352
9	08041700	Pine Island Bayou near Sour Lake, Texas	336	30.10605	94.33463
10	08065800	Bedias Creek near Madisonville, Texas	321	30.88472	95.77778
11	08066250	Trinity River near Goodrich, Texas	16,844	30.57215	94.94882
12	08066300	Menard Creek near Rye, Texas	152	30.48139	94.77972
13	08067000	Trinity River at Liberty, Texas	17,468	30.05772	94.81826
14	08067500	Cedar Bayou near Crosby, Texas	64.9	29.97272	94.98576
15	08067650	West Fork San Jacinto River below Lake Conroe near Conroe, Texas	451	30.34215	95.54300
16	08068000	West Fork San Jacinto River near Conroe, Texas	828	30.24466	95.45716
17	08068090	West Fork San Jacinto River above Lake Houston near Porter, Texas	962	30.08605	95.29993
18	08068275	Spring Creek near Tomball, Texas	186	30.11994	95.64606
19	08068325	Willow Creek near Tomball, Texas	41.0	30.10550	95.54661
20	08068390	Bear Branch at Research Boulevard, The Woodlands, Texas	15.4	30.19056	95.49111
21	08068400	Panther Branch at Gosling Road, The Woodlands, Texas	25.9	30.19194	95.48361
22	08068450	Panther Branch near Spring, Texas	34.5	30.13417	95.47750
23	08068500	Spring Creek near Spring, Texas	409	30.11050	95.43633
24	08068720	Cypress Creek at Katy-Hockley Road near Hockley, Texas	110	29.95022	95.80828
25	08068740	Cypress Creek at House-Hahl Road near Cypress, Texas	131	29.95911	95.71772
26	08068780	Little Cypress Creek near Cypress, Texas	41.0	30.01605	95.69745
27	08068800	Cypress Creek at Grant Road near Cypress, Texas	214	29.97356	95.59855
28	08068900	Cypress Creek at Stuebner-Airline Road near Westfield, Texas	248	30.00661	95.51189
29	08069000	Cypress Creek near Westfield, Texas	285	30.03578	95.42883
30	08070000	East Fork San Jacinto River near Cleveland, Texas	325	30.33660	95.10410
31	08070200	East Fork San Jacinto River near New Caney, Texas	388	30.14549	95.12438
32	08070500	Caney Creek near Splendora, Texas	105	30.25966	95.30244
33	08071000	Peach Creek at Splendora, Texas	117	30.23271	95.16827
34	08071280	Luce Bayou above Lake Houston near Huffman, Texas	218	30.10966	95.05993
35	08072300	Buffalo Bayou near Katy, Texas	63.3	29.74329	95.80690
36	08072730	Bear Creek near Barker, Texas	21.5	29.83078	95.68689
37	08072760	Langhan Creek at West Little York Road near Addicks, Texas	24.6	29.86694	95.64639
38	08073500	Buffalo Bayou near Addicks, Texas	277	29.76190	95.60578
39	08073600	Buffalo Bayou at West Belt Drive, Houston, Texas	290	29.76217	95.55772

6 Characterization of Peak Streamflows and Flood Inundations from Hurricane Harvey, 2017

Table 2. U.S. Geological Survey streamflow-gaging stations in southeast Texas with at least 15 years of record, no large data gaps in the period of record, and a 2017 annual peak streamflow ranking in the top five of all annual peaks for a given station that were used to calculate annual exceedance probabilities.—Continued

[mi², square miles]

Site identification number (fig. 2)	Station number	Station name	Drainage area (mi ²)	Latitude (decimal degrees)	Longitude (decimal degrees)
40	08073700	Buffalo Bayou at Piney Point, Texas	299	29.74690	95.52355
41	08074000	Buffalo Bayou at Houston, Texas	336	29.76023	95.40855
42	08074020	Whiteoak Bayou at Alabonson Road, Houston, Texas	34.5	29.87056	95.48028
43	08074150	Cole Creek at Deihl Road, Houston, Texas	7.50	29.85111	95.48778
44	08074250	Brickhouse Gully at Costa Rica Street, Houston, Texas	11.4	29.82778	95.46917
45	08074500	Whiteoak Bayou at Houston, Texas	95.1	29.77523	95.39716
46	08074800	Keegans Bayou at Roark Road near Houston, Texas	12.7	29.65662	95.56217
47	08075000	Brays Bayou at Houston, Texas	94.9	29.69717	95.41216
48	08075400	Sims Bayou at Hiram Clarke Street, Houston, Texas	20.2	29.61884	95.44605
49	08075500	Sims Bayou at Houston, Texas	63.0	29.67440	95.28938
50	08075730	Vince Bayou at Pasadena, Texas	8.26	29.69467	95.21632
51	08075770	Hunting Bayou at Interstate Highway 610, Houston, Texas	16.1	29.79328	95.26799
52	08075780	Greens Bayou at Cutten Road near Houston, Texas	8.65	29.94911	95.51966
53	08075900	Greens Bayou near US Highway 75 near Houston, Texas	36.6	29.95689	95.41799
54	08076000	Greens Bayou near Houston, Texas	68.7	29.91828	95.30688
55	08076180	Garners Bayou near Humble, Texas	31.0	29.93386	95.23396
56	08076500	Halls Bayou at Houston, Texas	28.7	29.86167	95.33472
57	08076700	Greens Bayou at Ley Road, Houston, Texas	182	29.83717	95.23327
58	08077600	Clear Creek near Friendswood, Texas	122	29.51746	95.17854
59	08110100	Davidson Creek near Lyons, Texas	195	30.41965	96.54025
60	08111700	Mill Creek near Bellville, Texas	376	29.88106	96.20524
61	08114000	Brazos River at Richmond, Texas	45,107	29.58246	95.75773
62	08116650	Brazos River near Rosharon, Texas	45,339	29.34969	95.58244
63	08117500	San Bernard River near Boling, Texas	727	29.31358	95.89384
64	08160400	Colorado River above La Grange, Texas	40,874	29.91245	96.90387
65	08160800	Redgate Creek near Columbus, Texas	17.3	29.79888	96.53194
66	08161000	Colorado River at Columbus, Texas	41,640	29.70635	96.53692
67	08162000	Colorado River at Wharton, Texas	42,003	29.30914	96.10385
68	08162500	Colorado River near Bay City, Texas	42,240	28.97415	96.01246
69	08164000	Lavaca River near Edna, Texas	817	28.95998	96.68637
70	08164300	Navidad River near Hallettsville, Texas	332	29.46691	96.81276
71	08164390	Navidad River at Strane Park near Edna, Texas	579	29.06554	96.67414
72	08164450	Sandy Creek near Ganado, Texas	289	29.16025	96.54636
73	08175800	Guadalupe River at Cuera, Texas	4,934	29.09053	97.32971
74	08176500	Guadalupe River at Victoria, Texas	5,198	28.79305	97.01304

Purpose and Scope

The purpose of this report is to document the characterization of peak streamflows and flood inundation of selected areas in southeastern Texas. The data collection methods, flood-peak magnitudes, and flood-inundation products generated by the USGS in support of the FEMA response-and-recovery operations following the August and September 2017 flood event in southeastern Texas caused by rainfall from Hurricane Harvey are described. This report includes (1) a description of the atmospheric conditions and the temporal and spatial patterns of rainfall that triggered the flooding and a description of the flood and its effects, (2) a description of the flagging and surveying of high-water marks (HWMs), (3) analysis of flood-peak magnitudes and their statistical probabilities at selected locations, (4) and geographic information system (GIS) analysis of HWM locations and elevations to produce flood-inundation maps (areal extent of the maximum depth of flooding) for five heavily flooded major river basins primarily in Texas, six smaller coastal basins, and coastal areas in Texas from Port Aransas to Matagorda Bay. Because one of the five heavily flooded river basins consists of the Sabine River and its tributaries, and the Sabine River forms part of the boundary between Texas and Louisiana, the study includes a small part of southwestern Louisiana. The wording and presentation of the material in this report are based on a previous USGS report (Watson and others, 2017); the contents of each section are modified from this previous report. In addition to the flooded river basins and areas described in this report, other river basins and areas also flooded as a result of Hurricane Harvey; documenting the flooding in other basins and areas affected by Hurricane Harvey is beyond the scope of this report.

Description of Study Area

The study area consists of five major river basins in southeastern Texas and a small part of southwestern Louisiana along the coast of the Gulf of Mexico, six smaller coastal basins that drain directly to the Gulf of Mexico, and coastal areas from Port Aransas to Matagorda Bay. Areas affected by flooding described within this report lie within the West Gulf Coastal Plain physiographic section (Fenneman, 1946; fig. 1). In general, the study area is characterized by coastal prairies that extend westward from the Texas and Louisiana border to Corpus Christi along the coast of the Gulf of Mexico and is primarily covered by heavy grasses. The soil in the study area is mostly heavy clay. The study area also extends into East Texas, which is covered by pine forests with some hardwood timber with sandy loam soils (Texas State Historical Association, 2018; Texas A&M Forest Service, 2018). Land-surface elevations within the study area range from about 0 to 602 feet (ft) relative to the North American Vertical Datum of 1988 (NAVD 88). The study area is primarily within two National Weather Service (NWS) climate divisions: East Texas

and Upper Coast (NOAA, 2017; fig. 1). According to data retrieved from the NWS National Climatic Data Center for the period from 1901 through 2013, mean annual precipitation for the East Texas climate division is 45.74 in., and mean annual precipitation for the Upper Coast climate division is 45.27 in. (NOAA, 2014).

Weather Conditions Before and During the Flood

On August 17, 2017, Harvey began as a tropical depression about 625 miles (mi) east of St. Vincent of the Lesser Antilles and became a weak tropical storm on August 18 near Barbados (Blake and Zelinsky, 2018). The storm then dissipated into a tropical wave over the Caribbean Sea on August 19 but re-formed into a tropical storm over the Bay of Campeche on August 23, eventually intensifying into a Category 4 hurricane on August 25. Harvey made landfall on August 25 as a Category 4 hurricane on the northern end of San Jose Island about 5 mi east of Rockport, Tex. (fig. 1) and made a second landfall on the mainland of Texas about 3 hours later. Harvey had sustained winds of 132 mi/h when it hit the northern end of San Jose Island and sustained winds of 121 mi/h when it hit the Texas mainland. Harvey weakened rapidly over land to a tropical storm after about 12 hours and maintained 40 mi/h winds for the next day or so (Blake and Zelinsky, 2018).

After making landfall, the storm made a slow loop beginning on August 26 and continuing into August 27 before drifting eastward and southeastward over the next couple of days. The center of the storm passed south of the Houston area, but heavy rains fell near a stationary front on the north and east sides of the storm. The center of the storm moved offshore over Matagorda Bay on August 28 and eventually turned to the north-northeast about 69 mi offshore from the Texas coast on August 29. Harvey continued on that path and eventually made landfall in southwestern Louisiana on August 30 with 46-mi/h sustained winds. The storm weakened from a tropical storm to a tropical depression late on August 30 and then moved northeastward over northern Louisiana. By August 31, the storm had moved over southeastern Arkansas, northern Mississippi, and central Tennessee. By the time the storm reached Tennessee, it had become an extratropical cyclone and eventually dissipated on September 2 in northern Kentucky (Blake and Zelinsky, 2018).

Harvey was the most significant rainfall event in United States history in scope and rainfall totals since rainfall records began during the 1880s. For the period from August 25 through September 1, 2017, the highest rainfall total from the storm at a single location was 60.58 in. near Nederland, Tex. (table 1). A location near Groves, Tex. (fig. 1) also reported 60.54 in. of rain during the same period (table 1; Blake and Zelinsky, 2018). The record rainfall amounts of

60.58 and 60.54 inches listed in table 1 are from Jefferson County Drainage District rain gages, which were probably not used by the National Weather Service to create the maps depicting rainfall amounts in the study area. To create maps of rainfall amounts, the National Weather Service averages rainfall over large areas, which could also account for discrepancies between the maximum rainfall amounts depicted in figures 1–2 and the individual point values exceeding 60 inches of rain listed in table 1. The previous record storm total for the continental United States was 48.00 in. of rain near Medina, Tex., in 1978 which was associated with Tropical Storm Amelia. During Harvey, 20 NOAA meteorological stations reported rainfall totals in excess of 48.00 in. across southeastern Texas for the period from August 25 through September 1, 2017 (table 1; Blake and Zelinsky, 2018). Not only were Harvey's rainfall totals exceptional, but the areal extent of heavy rainfall was also larger than the areal extents of previous events with rainfall totals exceeding 15 in. (Blake and Zelinsky, 2018).

The heavy rainfall led to widespread flooding and record streamflows. In Texas, 74 USGS streamflow-gaging stations with at least 15 years of record (table 2) had annual peak streamflows for the 2017 water year¹ resulting from Harvey that ranked among the top five of all annual peak streamflows recorded for that station (table 3). For 40 of these 74 streamflow-gaging stations (54 percent), the 2017 annual peak streamflow ranked as the largest ever recorded for the station (table 3).

Harvey also produced 57 tornadoes (as reported by October 1, 2017) in Texas, Louisiana, Mississippi, Alabama, and Tennessee, with about half of them occurring near and south of the Houston metropolitan area (Blake and Zelinsky, 2018). Most of the tornadoes were relatively weak and resulted in no fatalities.

Methods

The methods used to identify, document, and reference HWMs resulting from flooding as well as the methods used to create flood-inundation maps from HWMs are described in this section. Also discussed are the methods by which the estimation of flood magnitude and frequency were developed through analysis of the annual peak streamflows at 74 streamflow-gaging stations operated by the USGS. The USGS collects streamflow data at more than 8,000 streamflow-gaging stations nationwide in cooperation with local, state, and Federal agencies. This includes more than 600 streamflow-gaging stations currently (2018) operating in Texas. Collection

of streamflow data documents the extent and effects of flooding. Streamflow data collected before and during flooding are vital because they can provide advanced flood warning, forecasts of the extent and potential effects of flooding, and information useful in optimizing allocation of emergency management resources to the most severely affected areas. All streamflow data used in support of this report can be accessed from the USGS National Water Information System (USGS, 2018a).

Collection of High-Water Mark Data

HWMs are the evidence of the highest water levels during a flood and provide valuable data for understanding flood events (Koenig and others, 2016). The USGS followed the guidance provided by Koenig and others (2016) for identification and documentation of HWMs. The best HWMs are formed from small seeds or floating debris carried by floodwaters that adhere to smooth surfaces or lodge in tree bark to form a distinct line. Stain lines on buildings, fences, and other structures also provide excellent marks. HWMs are best identified immediately following the peak stage of a flood event because time and weather (wind, rain, and sun) may blow, wash, or fade away the evidence of the peak water line. Care was taken to identify HWMs as far from the main channel as feasible, where velocities generally are slower and where wave action and pileup or drawdown effects of fast-moving waters are minimized. Information about the HWMs identified by the USGS for this flood event was made available through the USGS Short-Term Network (STN) (USGS, 2018b), which is an online interface created to facilitate the dissemination of field data. Additional information, including a download portal for HWM information from the Flood Event Viewer, is available from the USGS Hurricane Harvey web page at <https://www.usgs.gov/special-topic/hurricane-harvey> (USGS, 2018c).

Identification of HWMs by the USGS began on September 2, 2017, and continued through October 5, 2017. After an acceptable HWM was found, a more permanent identification mark was established, such as a Parker-Kalon nail with a disk, a stake, a chiseled mark, or a paint line. Written descriptions, sketches, photographs, and Global Positioning System (GPS) horizontal measurements obtained with a hand-held GPS unit were made so the marks could easily be found later and surveyed to the standard vertical datum, NAVD 88. USGS field crews surveyed 2,123 HWMs to obtain water-surface elevations, in feet above NAVD 88. In some locations, several water-surface elevations were averaged to obtain 1 water-surface elevation, resulting in 1,258 water-surface elevations. The distance of the HWMs above the land surface was also recorded in feet for all of the HWMs.

¹The water year is the annual period from October 1 through September 30 and is designated by the year in which the period ends. For example, the 2017 water year is from October 1, 2016, through September 30, 2017.

Table 3. Peak gage heights, peak streamflows, and estimated annual exceedance probabilities for the August and September 2017 Hurricane Harvey-related flood event at 74 selected U.S. Geological Survey streamflow-gaging stations in southeastern Texas.[ft, feet; ft³/s, cubic feet per second; AEP, annual exceedance probability]

Site identi- fication number (fig. 2)	Station number	Peak streamflow for August 2017 flood				Number of annual peak streamflows in period of record	AEP for observed August 2017 flood		
		Date of peak stream- flow	Peak gage height (ft)	Peak streamflow (ft ³ /s)	Rank of peak streamflow among all annual peak streamflows		Estimate (percent)	66.7 percent confidence interval	
								Lower (percent)	Upper (percent)
1	08026000	9/1/2017	46.29	84,900	5	62	4.0	4.7	11.1
2	08028500	9/2/2017	38.93	113,000	3	93	2.3	1.5	4.8
3	08029500	8/30/2017	21.08	39,500	2	66	1.0	1.1	4.8
4	08030500	9/2/2017	31.60	161,000	2	105	0.4	0.7	3.0
5	08031000	8/30/2017	26.85	26,500	1	47	0.3	0.4	3.7
6	08039100	8/30/2017	17.49	15,700	4	60	5.4	3.6	9.5
7	08040600	8/31/2017	80.70	91,000	2	68	1.0	1.1	4.7
8	08041500	8/30/2017	35.96	182,000	1	82	0.3	0.2	2.2
9	08041700	8/30/2017	39.68	50,500	1	50	1.0	0.4	3.5
10	08065800	8/28/2017	26.03	38,700	3	50	3.8	2.8	8.9
11	08066250	8/29/2017	48.34	110,000	2	52	2.7	1.4	6.1
12	08066300	8/29/2017	36.11	15,200	1	52	1.9	0.4	3.4
13	08067000	8/31/2017	32.70	126,100	2	76	1.4	1.0	4.2
14	08067500	8/28/2017	59.06	10,600	1	46	0.3	0.4	3.8
15	08067650	8/28/2017	46.12	75,400	1	45	1.5	0.4	3.9
16	08068000	8/29/2017	126.93	122,000	1	83	0.8	0.2	2.1
17	08068090	8/29/2017	94.87	131,000	1	33	2.4	0.6	5.3
18	08068275	8/28/2017	166.38	48,900	1	18	4.5	1.0	9.5
19	08068325	8/28/2017	133.87	11,100	1	27	1.8	0.7	6.4
20	08068390	8/28/2017	140.27	3,660	3	18	14.0	7.9	23.6
21	08068400	8/28/2017	137.49	6,300	4	18	9.7	12.1	29.9
22	08068450	8/28/2018	117.12	12,500	2	25	3.4	2.9	12.4
23	08068500	8/28/2017	111.52	78,400	2	80	1.1	0.9	4.0
24	08068720	8/28/2017	162.85	12,800	1	42	0.5	0.4	4.2
25	08068740	8/28/2017	149.30	22,600	1	43	1.1	0.4	4.1
26	08068780	8/28/2017	161.23	9,140	2	35	2.3	2.1	8.9
27	08068800	8/28/2017	129.97	17,500	2	35	1.9	2.1	8.9
28	08068900	8/28/2017	113.82	23,100	1	31	1.3	0.6	5.6
29	08069000	8/28/2017	97.12	31,500	1	75	0.5	0.2	2.4
30	08070000	8/28/2017	27.17	109,000	1	79	0.8	0.2	2.2
31	08070200	8/29/2017	81.15	120,000	1	33	0.5	0.6	5.3
32	08070500	8/28/2017	26.63	21,100	4	74	3.3	2.9	7.7
33	08071000	8/28/2017	25.77	77,000	1	54	0.8	0.3	3.3
34	08071280	8/29/2017	37.86	32,800	1	33	2.6	0.6	5.3
35	08072300	8/28/2017	118.28	17,900	1	40	0.4	0.5	4.4
36	08072730	8/27/2017	114.71	15,700	2	40	3.7	1.8	7.9
37	08072760	8/27/2017	111.85	9,000	3	40	6.2	3.5	11.0
38	08073500	8/30/2017	77.31	13,800	1	73	0.4	0.2	2.4

10 Characterization of Peak Streamflows and Flood Inundations from Hurricane Harvey, 2017

Table 3. Peak gage heights, peak streamflows, and estimated annual exceedance probabilities for the August and September 2017 Hurricane Harvey-related flood event at 74 selected U.S. Geological Survey streamflow-gaging stations in southeastern Texas.— Continued

[ft, feet; ft³/s, cubic feet per second; AEP, annual exceedance probability]

Site identi- fication number (fig. 2)	Station number	Peak streamflow for August 2017 flood				Number of annual peak streamflows in period of record	AEP for observed August 2017 flood		
		Date of peak stream- flow	Peak gage height (ft)	Peak streamflow (ft ³ /s)	Rank of peak streamflow among all annual peak streamflows		Estimate (percent)	66.7 percent confidence interval	
								Lower (percent)	Upper (percent)
39	08073600	8/31/2017	71.22	14,600	1	46	0.4	0.4	3.8
40	08073700	8/31/2017	62.84	15,000	1	47	0.5	0.4	3.7
41	08074000	8/28/2017	41.90	36,400	1 ²	83	0.3	0.9	3.8
42	08074020	8/27/2017	77.84	15,500	1	34	3.1	0.5	5.1
43	08074150	8/27/2017	74.58	2,620	5	51	8.1	5.7	13.4
44	08074250	8/27/2017	66.97	11,800	2	47	1.4	1.6	6.7
45	08074500	8/27/2017	44.31	50,600	1	83	<0.2	0.2	2.1
46	08074800	8/27/2017	75.21	9,870	1	52	0.6	0.4	3.4
47	08075000	8/27/2017	45.67	35,200	1	83	2.5	0.2	2.1
48	08075400	8/27/2017	46.78	13,500	1	53	0.7	0.3	3.3
49	08075500	8/27/2017	26.56	39,700	1	65	0.3	0.3	2.7
50	08075730	8/27/2017	22.32	8,430	1	46	0.8	0.4	3.8
51	08075770	8/27/2017	37.12	6,680	1	54	0.6	0.3	3.3
52	08075780	8/27/2017	111.84	5,840	1	53	4.3	0.3	3.3
53	08075900	8/27/2017	85.84	12,000	4	52	4.7	4.1	10.9
54	08076000	8/27/2017	62.88	26,400	2	65	1.3	1.1	4.9
55	08076180	8/28/2017	57.92	24,900	1	31	1.0	0.6	5.6
56	08076500	8/28/2017	57.54	5,550	2	65	2.8	1.1	4.9
57	08076700	8/28/2017	44.85	128,000	1	45	0.5	0.4	3.9
58	08077600	8/29/2017	24.25	44,100	1	21	0.5	0.9	8.2
59	08110100	8/28/2017	19.47	23,500	2	55	2.5	1.3	5.8
60	08111700	8/28/2017	22.49	73,800	2	47	1.5	1.6	6.7
61	08114000	9/1/2017	55.19	122,000	2	99	0.9	0.7	3.2
62	08116650	8/29/2017	52.65	133,000	1	48	0.4	0.4	3.7
63	08117500	8/31/2017	43.79	54,500	1	63	0.2	0.3	2.8
64	08160400	8/28/2017	54.14	118,000	1	29	5.2	0.6	6.0
65	08160800	8/27/2017	26.60	5,290	3	56	6.8	2.5	8.0
66	08161000	8/29/2017	48.13	165,000	3	104	1.1	1.4	4.3
67	08162000	8/31/2017	50.47	93,600	4	87	3.7	2.5	6.6
68	08162500	9/2/2017	46.16	89,000	1	71	1.6	0.3	2.5
69	08164000	8/29/2017	32.53	74,300	4	80	3.2	2.7	7.2
70	08164300	8/28/2017	36.38	61,900	1	56	0.6	0.3	3.1
71	08164390	8/29/2017	31.28	26,000	1	20	6.4	0.9	8.6
72	08164450	8/29/2017	25.84	20,500	3	40	7.9	3.5	11.0
73	08175800	8/29/2017	44.36	178,000	2	54	3.4	1.4	5.9
74	08176500	8/30/2017	31.30	86,500	5	83	8.0	3.5	8.4

¹Hurricane Harvey peak streamflow ranked second behind a historic peak of record.

During the mapping process, the HWMs used to create flood-inundation maps (Watson and others, 2018) were checked for location and elevation accuracy by comparing field note diagrams and descriptions to aerial photography and detailed street and parcel maps. If the location could not be determined accurately or if the elevation was substantially different from the elevations of other HWMs in the area, the HWM was not used. Also, some HWMs were not used because they were the result of localized flooding of small areas and did not represent the water-surface elevation of the surrounding area.

Flood-Inundation Mapping

Nineteen flood-inundation maps in 11 river and coastal basins were created by using GIS for areas near rivers that flooded as a result of Harvey in southeastern Texas and southwestern Louisiana (fig. 3). The flood-inundation maps estimate the areal extent of the maximum depth of flooding that corresponds to the HWMs identified and surveyed by USGS field crews following the flood event. The waterbody, reach length, and number of HWMs used to generate the flood-inundation maps are summarized (table 4).

The first step in the generation of the flood-inundation maps was the creation of a flood-elevation raster surface. GIS surfaces documenting the areal extent of the maximum depth of flooding were created independently for each area that was mapped by using the HWM elevations, cross sections across the direction of flow at the HWMs and streamflow-gaging stations, and a GIS interpolation technique—the ArcGIS Topo to Raster tool (<http://pro.arcgis.com/en/pro-app/tool-reference/3d-analyst/how-topo-to-raster-works.htm>, accessed February 13, 2018) as described by Musser and others (2016). A different method was used in the coastal areas with relatively low topography and large areas of overland flooding. This interpolation method used the HWM elevations as points rather than cross sections and interpolated between these elevations to generate the flood-elevation surface by using the ArcGIS Topo to Raster tool with the point interpolation procedure. A geographic limit was placed on the extent of the generated surface on the basis of the distribution of HWMs and an understanding of the natural hydrologic flow in each area that was mapped.

The flood-elevation surface that was created by using GIS interpolation was then combined with digital elevation model (DEM) data, derived from light detection and ranging (lidar) data, with cell sizes of 1.4–3.0 meters (USGS Lidar Point Cloud TX Neches, USGS, The National Map, 2018; Texas Natural Resources Information System, 2006, 2007, 2008, 2009, 2010, 2011a–d, 2012, 2013, 2014, 2016, 2017). A DEM is digital point representation of a surface; in this instance, the DEM is a representation of the earth's surface in the study area and mimics the topography of the land. An inundated area was depicted where the interpolated flood-elevation surface was higher than the DEM land surface. The maximum depth of

flooding was determined as the difference between the flood-elevation surface and the DEM land surface. For this study, the flood-inundation surfaces were not modified to show any bridges that were not inundated. Our modeling methods did not use a hydraulic analysis, so we cannot definitively show whether a bridge was inundated or not.

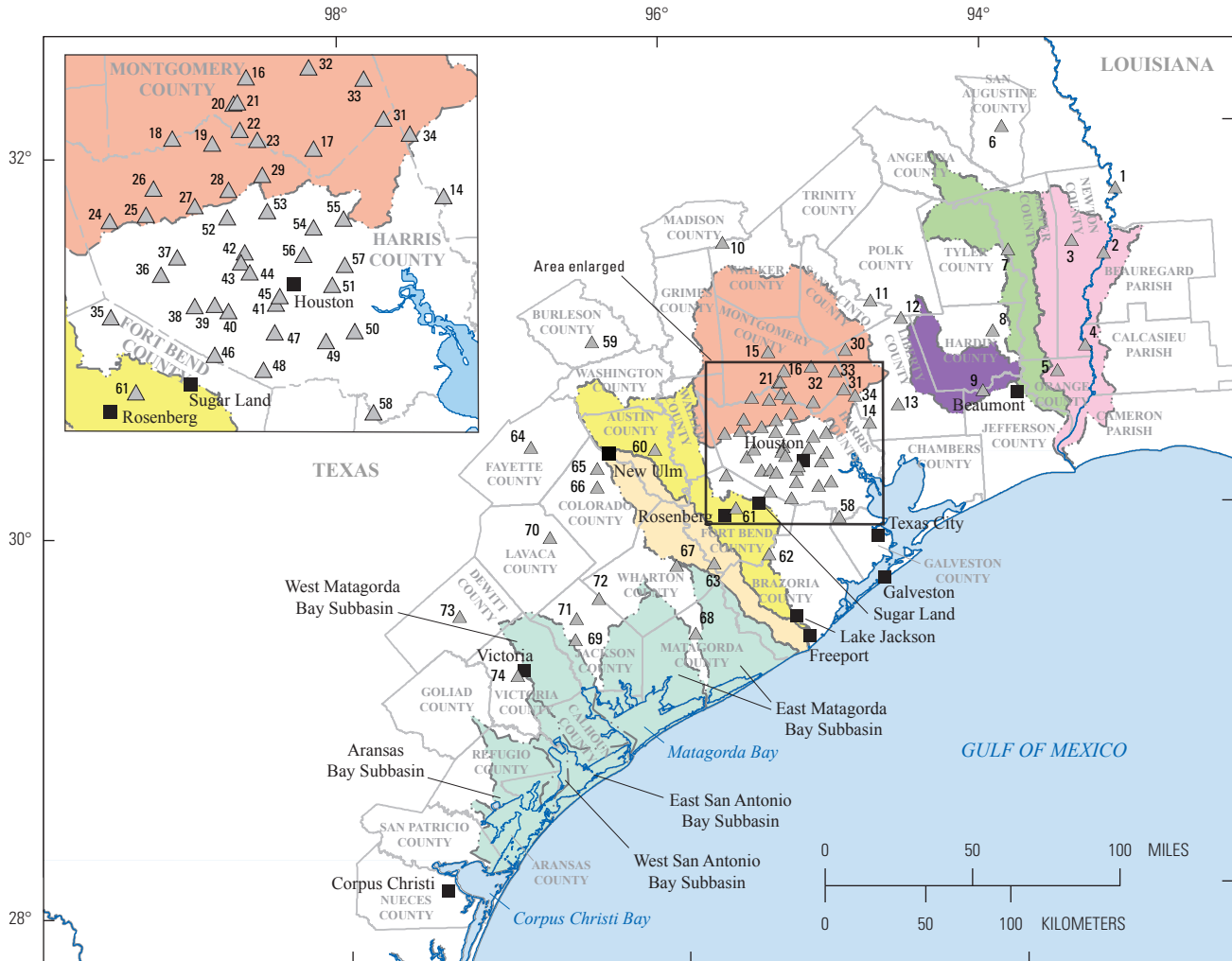
The flood-elevation interpolation method used to develop the coastal water-surface elevation layer used the HWM and USGS streamflow-gaging station peak stage water-surface elevation values as points and interpolated between these elevations to generate the water-surface elevation by using the ArcGIS Topo to Raster tool with the point interpolation procedure (<http://pro.arcgis.com/en/pro-app/tool-reference/3d-analyst/how-topo-to-raster-works.htm>; Esri, 2017). This approach was used when the flooded area was adjacent to a large, low-gradient body of water, such as a swamp, or when the flooded area was a coastal community on the Gulf of Mexico.

Uncertainties in the mapped extent of the maximum depth of flooding exist within the maps because of the mapping methods used and the number and spatial distribution of HWMs in a given mapped reach. Hydraulic models were not used to determine the extent or depth of flood inundation. Without hydraulic models, changes in land-surface features in flood plains, the timing of the flooding that may have occurred from some of the smaller inflow tributaries versus the larger main stem tributaries, and the intermingling flows from adjacent streams are not taken into account. In locations where HWMs are spaced farther apart, there is a greater possibility of decreased accuracy of spatial interpretation of the extent of the maximum depth of flood inundation. Within a given mapped area, some extrapolation was performed beyond the most upstream and downstream HWMs. In many cases, the mapped boundary was extended to some anthropogenic structure, such as a road or bridge crossing.

Flood Exceedance Probabilities of Peak Streamflows

After a major flood, emergency managers and water resources engineers often need to know the expected frequency of peak streamflow for the streamflow magnitudes observed during the event. Flood-frequency analyses for streamflow-gaging stations with sufficient record (defined as greater than or equal to 15 years for the purposes of this report) can provide insight into the occurrence or likelihood of peak streamflows of varying magnitudes. The annual exceedance probability (AEP) for a particular location is the probability of that streamflow being equaled or exceeded during a given water year and is determined from the existing annual peak streamflow data for a streamflow-gaging station. For example, an AEP of 0.01 means there is a 1-percent (AEP \times 100) chance that a specific peak streamflow will occur at a given location in a given year. Stated another way, the odds are 1 in 100 that the indicated streamflow will be

12 Characterization of Peak Streamflows and Flood Inundations from Hurricane Harvey, 2017



Base modified from U.S. Geological Survey digital data
 Albers Equal Area Projection, Texas Centric Mapping System
 North American Datum of 1983 (2011)

- EXPLANATION**
- Lower Brazos Basin
 - Lower Neches Subbasin
 - Pine Island Bayou Subbasin
 - Sabine Basin
 - San Bernard Coastal Basin
 - San Jacinto Basin
 - Coastal basins—East Matagorda Bay Subbasin, West Matagorda Bay Subbasin, East San Antonio Bay Subbasin, West San Antonio Bay Subbasin, and Aransas Bay Subbasin
 - Basin boundary
 - Subbasin boundary
 - U.S. Geological Survey streamflow-gaging station and site identification number—Used for annual exceedance probability calculation, see table 2

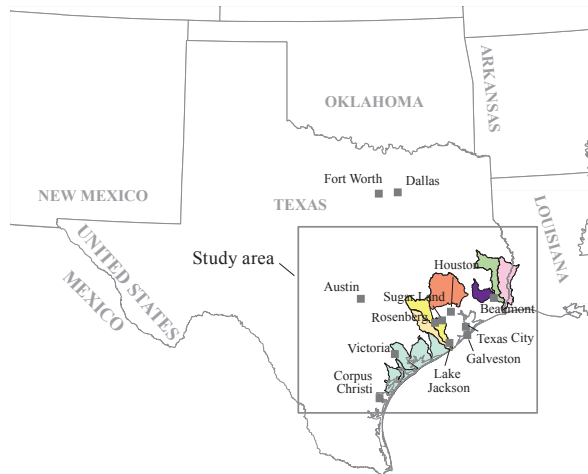


Figure 3. Locations of U.S. Geological Survey streamflow-gaging stations, selected cities and counties, parishes, and river basins within the study area in southeastern Texas and southwestern Louisiana.

Table 4. Counties, parishes, waterbodies, reach lengths, and number of high-water marks used to generate flood-inundation maps.

Texas County/ Louisiana Parish ¹	Waterbody	Reach length (miles) ²	Number of high- water marks
Waller, Austin, Fort Bend, and Brazoria	Brazos River	171	46
Orange, Jasper, Hardin, Jefferson, and Tyler	Neches River	131	33
Liberty, Hardin, Jefferson, and Orange	Pine Island Bayou, tributary to the Neches River	68	34
Jasper, Newton, Orange, Jefferson, Beauregard, Calcasieu, and Cameron	Sabine River	131	43
Jasper and Newton	Big Cow Creek, tributary to the Sabine River	37	8
Jasper, Newton, and Orange	Cow Bayou, tributary to the Sabine River	23	19
Colorado, Austin, Wharton, Fort Bend, and Brazoria	San Bernard River	99	34
Waller, Harris, Montgomery, San Jacinto, and Liberty	San Jacinto River and tributaries	403	106
Matagorda, Jackson, Calhoun, Victoria, Refugio, San Patricio, and Aransas	Coastal Basins (including Peyton Creek, Big Boggy Creek, Little Boggy Creek, Tres Palacios River, East Carancahua Creek, West Carancahua Creek, and Keller Creek)	234	129

¹Bold-faced names are parishes in Louisiana.

²Indicates total reach length mapped within a basin computed as the sum of the main stem and tributaries.

equaled or exceeded in a given year. The traditional concept of recurrence interval is directly related to the AEP. By definition, the recurrence interval (in years) is equal to 1 divided by the AEP. For example, the AEP of 0.01 (or 1 percent) corresponds to the 100-year flood (Holmes and Dinicola, 2010).

During August and September 2017, USGS personnel made more than 180 streamflow measurements in the study area by direct methods (Rantz and others, 1982a; Turnipseed and Sauer, 2010) and indirect methods (Benson and Dalrymple, 1967; Rantz and others, 1982b) at 97 locations. Many of the streamflow measurements were made to verify the accuracy of the stage-streamflow rating curve or to extend the stage-streamflow rating curve for a given streamflow-gaging station (Rantz and others, 1982a). The stage-streamflow rating curve for a given streamflow-gaging station is used to calculate instantaneous streamflow values for given stage values, which in turn are used to populate USGS annual peak streamflow files. Streamflow-gaging stations with the longest annual peak streamflow records are considered the most reliable for estimating AEPs.

The August and September 2017 peak streamflows were analyzed by using the PeakFQ software (Flynn and others, 2006) following guidance provided in USGS Office of Surface Water Technical Memorandum 2013.01 (Mason, 2012). For

selected streamflow-gaging stations, AEPs corresponding to peak streamflows that occurred during the August and September 2017 flood and streamflows associated with selected AEPs (1, 0.5, and 0.2 percent; table 5) were estimated by using the Expected Moments Algorithm (Cohn and others, 1997, 2001) in the USGS PeakFQ software (Flynn and others, 2006; USGS, 2018d). The Interagency Advisory Committee on Water Data (IACWD) provides standard methods for computing peak streamflow frequency in a recently (2018) published document referred to as Bulletin 17C (England and others, 2018). Bulletin 17C is an update to Bulletin 17B (IACWD, 1982). Flood computation equations and algorithms in Bulletin 17C have been implemented in the PeakFQ software (Veilleux and others, 2014; USGS, 2018d). The PeakFQ software includes an updated version of the Expected Moments Algorithm, which allows for the incorporation of more complicated or subjective measurements such as paleo-hydrology, interval peaks, and sophisticated gap-infill for years of missing annual peak streamflow records. The PeakFQ software was updated to include the multiple Grubbs-Beck low outlier test, which is capable of identifying potentially influencing low floods. The multiple Grubbs-Beck low outlier test is an improvement over the single Grubbs-Beck test (Grubbs and Beck, 1972; England and others, 2018).

14 Characterization of Peak Streamflows and Flood Inundations from Hurricane Harvey, 2017

Table 5. Site identification number, station number, and expected peak streamflows for selected annual exceedance probabilities with 95 percent confidence intervals at 74 selected U.S. Geological Survey streamflow-gaging stations in southeastern Texas.

[ft³/s, cubic feet per second; AEP, annual exceedance probability]

Site identi- fication number (fig. 2)	Station number	Expected peak streamflows for selected AEP with 95 percent confidence intervals (ft ³ /s)								
		1 percent AEP (100-year recurrence)			0.5 percent AEP (200-year recurrence)			0.2 percent AEP (500-year recurrence)		
		Estimate	95 percent confidence interval		Estimate	95 percent confidence interval		Estimate	95 percent confidence interval	
			Lower	Upper		Lower	Upper		Lower	Upper
1	08026000	140,000	103,000	276,000	176,000	123,000	425,000	234,000	153,000	762,000
2	08028500	141,000	110,000	222,000	168,000	126,000	294,000	208,000	148,000	419,000
3	08029500	39,100	22,700	135,000	54,700	29,200	267,000	83,300	39,600	672,000
4	08030500	138,000	113,000	193,000	157,000	124,000	234,000	182,000	137,000	298,000
5	08031000	12,000	5,880	62,100	17,900	7,380	157,000	29,800	9,720	572,000
6	08039100	26,700	18,000	56,600	31,800	20,200	77,500	39,100	22,700	116,000
7	08040600	90,800	65,500	166,000	111,000	76,000	238,000	142,000	91,200	386,000
8	08041500	106,000	66,600	289,000	140,000	82,100	490,000	198,000	104,000	973,000
9	08041700	50,700	28,900	263,000	68,600	36,000	489,000	99,800	46,800	1,060,000
10	08065800	55,400	39,700	92,000	64,300	43,800	119,000	75,900	48,200	163,000
11	08066250	126,000	106,000	174,000	137,000	113,000	206,000	150,000	121,000	256,000
12	08066300	18,500	12,900	40,100	22,800	15,100	61,100	29,100	17,900	106,000
13	08067000	132,000	108,000	197,000	148,000	118,000	244,000	169,000	130,000	322,000
14	08067500	8,290	6,270	15,000	9,410	6,820	18,900	11,000	7,480	25,500
15	08067650	97,700	39,000	1,840,000	158,000	54,100	5,360,000	292,000	80,500	22,400,000
16	08068000	111,000	74,400	217,000	136,000	85,100	304,000	169,000	97,000	464,000
17	08068090	196,000	98,200	752,000	263,000	122,000	1,240,000	374,000	155,000	2,340,000
18	08068275	109,000	42,100	870,000	147,000	52,300	1,580,000	212,000	66,500	3,350,000
19	08068325	14,200	7,580	48,600	18,700	9,290	78,100	26,100	11,700	143,000
20	08068390	8,600	5,160	26,700	10,200	5,830	37,200	12,500	6,700	56,700
21	08068400	15,100	8,260	61,200	18,800	9,690	93,900	24,700	11,700	163,000
22	08068450	24,600	11,200	288,000	34,500	14,400	598,000	51,900	19,400	1,490,000
23	08068500	80,100	49,400	317,000	109,000	62,100	608,000	160,000	81,400	1,330,000
24	08068720	9,790	5,730	49,400	12,700	6,880	84,400	17,500	8,510	171,000
25	08068740	23,800	9,540	163,000	36,800	12,300	441,000	64,700	16,700	1,780,000
26	08068780	12,200	7,270	32,700	15,200	8,530	47,400	19,700	10,200	76,000
27	08068800	21,700	13,400	77,600	26,900	15,400	125,000	34,700	18,200	233,000
28	08068900	24,600	16,600	52,400	29,200	18,800	69,900	35,700	21,700	101,000
29	08069000	26,200	19,700	50,300	31,100	22,400	70,700	38,400	25,900	110,000
30	08070000	95,900	55,900	295,000	132,000	70,600	519,000	194,000	92,300	1,070,000
31	08070200	86,900	42,600	336,000	121,000	54,400	587,000	180,000	72,600	1,200,000
32	08070500	39,800	22,700	184,000	56,600	29,500	398,000	88,300	40,800	947,000
33	08071000	63,000	27,600	367,000	102,000	39,700	880,000	186,000	60,600	2,730,000
34	08071280	49,300	25,500	360,000	64,500	30,600	645,000	89,100	37,300	1,390,000
35	08072300	12,300	6,920	69,300	16,300	8,240	133,000	23,400	10,200	317,000
36	08072730	35,500	15,800	433,000	53,200	21,100	999,000	88,300	29,800	3,000,000
37	08072760	21,700	11,600	118,000	29,100	14,300	235,000	41,700	18,300	516,000

Table 5. Site identification number, station number, and expected peak streamflows for selected annual exceedance probabilities with 95 percent confidence intervals at 74 selected U.S. Geological Survey streamflow-gaging stations in southeastern Texas.—Continued[ft³/s, cubic feet per second; AEP, annual exceedance probability]

Site identi- fication number (fig. 2)	Station number	Expected peak streamflows for selected AEP with 95 percent confidence intervals (ft ³ /s)								
		1 percent AEP (100-year recurrence)			0.5 percent AEP (200-year recurrence)			0.2 percent AEP (500-year recurrence)		
		Estimate	95 percent confidence interval		Estimate	95 percent confidence interval		Estimate	95 percent confidence interval	
			Lower	Upper		Lower	Upper		Lower	Upper
38	08073500	10,900	8,340	19,200	12,700	9,360	25,300	15,300	10,700	36,300
39	08073600	11,700	8,580	30,300	13,800	9,650	42,400	16,900	11,100	66,200
40	08073700	12,500	9,180	33,500	14,800	10,400	48,200	18,300	11,900	78,100
41	08074000	26,900	20,100	48,700	32,000	23,000	66,000	39,700	26,700	97,800
42	08074020	19,200	13,800	36,300	21,600	14,600	45,000	24,700	15,400	59,200
43	08074150	3,860	3,000	6,130	4,230	3,150	7,330	4,690	3,300	9,220
44	08074250	12,400	9,520	22,700	14,000	10,400	29,500	16,000	11,300	41,600
45	08074500	33,900	26,000	55,000	38,900	28,700	70,200	45,600	31,800	95,800
46	08074800	8,660	6,330	14,700	10,000	7,080	18,500	12,000	8,040	24,700
47	08075000	40,000	32,400	56,300	43,100	33,800	65,500	46,500	35,000	79,300
48	08075400	12,500	9,120	24,900	14,500	10,100	33,200	17,300	11,300	47,900
49	08075500	30,300	21,900	59,000	35,600	24,400	78,900	43,200	27,500	114,000
50	08075730	8,040	6,040	19,000	9,320	6,730	25,600	11,200	7,660	37,800
51	08075770	6,200	4,860	10,200	6,830	5,170	12,500	7,620	5,500	16,200
52	08075780	12,700	6,860	67,100	17,600	8,740	141,000	26,600	11,700	329,000
53	08075900	16,900	12,600	41,100	19,300	13,900	53,600	22,600	15,600	74,400
54	08076000	27,900	19,400	69,300	34,400	22,500	106,000	44,400	27,000	186,000
55	08076180	24,700	14,200	152,000	32,100	17,000	271,000	44,600	21,200	585,000
56	08076500	6,690	5,410	10,900	7,500	5,880	13,600	8,630	6,460	18,100
57	08076700	91,000	50,100	568,000	124,000	61,700	1,130,000	185,000	79,900	2,820,000
58	08077600	32,700	18,600	154,000	43,000	21,600	343,000	61,300	25,800	893,000
59	08110100	31,700	21,100	66,200	38,500	24,500	92,600	48,200	28,800	143,000
60	08111700	84,500	49,800	472,000	109,000	60,500	818,000	149,000	75,700	1,610,000
61	08114000	121,000	109,000	144,000	128,000	114,000	155,000	136,000	120,000	170,000
62	08116650	117,000	98,500	152,000	129,000	107,000	176,000	146,000	117,000	212,000
63	08117500	36,200	27,000	72,300	44,000	31,300	106,000	55,800	37,100	177,000
64	08160400	203,000	118,000	574,000	251,000	137,000	821,000	324,000	164,000	1,290,000
65	08160800	8,460	6,310	16,300	9,670	6,950	21,800	11,300	7,700	32,300
66	08161000	169,000	134,000	245,000	196,000	149,000	305,000	233,000	166,000	402,000
67	08162000	135,000	102,000	233,000	160,000	116,000	314,000	194,000	133,000	460,000
68	08162500	94,100	79,800	118,000	102,000	85,600	133,000	111,000	91,400	156,000
69	08164000	118,000	76,600	275,000	151,000	91,900	419,000	204,000	113,000	717,000
70	08164300	55,700	40,700	93,200	63,300	44,500	119,000	72,900	48,300	163,000
71	08164390	48,500	27,300	152,000	58,500	31,300	215,000	73,000	36,400	331,000
72	08164450	54,500	30,200	347,000	73,000	37,200	647,000	105,000	47,500	1,470,000
73	08175800	363,000	182,000	2,680,000	532,000	240,000	5,980,000	858,000	337,000	15,800,000
74	08176500	240,000	149,000	614,000	320,000	184,000	987,000	454,000	237,000	1,810,000

The PeakFQ software uses the three-parameter, log-Pearson type III (LPIII) probability distribution; the use of this distribution for flood analysis is a standard practice in the United States (IACWD, 1982). The first and second parameters of the LPIII are the arithmetic mean and standard deviation, and the third parameter of the LPIII is the sample skew. The sample skew was computed for the data for most streamflow-gaging station locations by using the “station skew” option, which uses the LPIII calculated skew without any regional weighting. If a station lacked information on natural peak streamflows, the skew calculated by PeakFQ was weighted by a regional skew value. The following situations required the use of a regionally weighted skew value: (1) the period of record was too short for a reliable LPIII fitted distribution (typically less than 40 years); (2) the periods of record were extensively truncated because of low outlier thresholds (for example, a large amount of the peak-flow record consisted of nonflood peak events that were removed by the multiple Grubbs-Beck low outlier test, leaving a much shorter period of record available for analysis); or (3) the peak-flow record was visibly affected by upstream dams or other streamflow regulation. Regional skew information was obtained from Judd and others (1996), who calculated regional regression equations for natural stream basins in Texas, thus providing a more focused analysis than the regional skew values presented in Bulletin 17B. The weighted streamflow estimates were then used to determine the AEP associated with the August and September 2017 peak streamflow.

Estimated Magnitudes and Flood Exceedance Probabilities of Peak Streamflows

The number of years of peak streamflow record for the 74 analyzed streamflow-gaging stations ranged from 18 to 105, with a mean of 55 years. New record peak streamflows were measured at 40 of the 74 USGS streamflow-gaging stations (table 3). Peak streamflows ranked second or third among the highest peaks of record measured at another 25 streamflow-gaging stations. At the nine remaining streamflow-gaging stations, peak streamflows ranked fourth or fifth among the highest peaks of record measured at these stations. The AEP estimates for the analyzed streamflow-gaging stations ranged from less than 0.2 to 14.0 percent. The expected peak streamflows for selected AEPs (1, 0.5, and 0.2 percent) with 95 percent confidence intervals at the 74 streamflow-gaging stations are provided in table 5.

Flood-Inundation Maps

Nineteen flood-inundation maps were created for flooded areas in southeastern Texas and a small part of southwestern Louisiana (figs. 3–22). Each map presents the areal extent of the floodwaters along affected reaches. The HWMs used to create the inundation maps and associated information can be accessed at the USGS STN website (USGS, 2018b) and are provided in Watson and others (2018). Digital datasets of the inundation area, modeling boundary, water-depth rasters, and final map products are available for download at <https://doi.org/10.5066/F7VH5N3N> (Watson and others, 2018). The areas covered by the specific flood-inundation maps are described in the following sections. All reported peak-stage data obtained from USGS streamflow-gaging stations (U.S. Geological Survey, 2018a) for use in this report represent final approved data unless explicitly stated as provisional data.

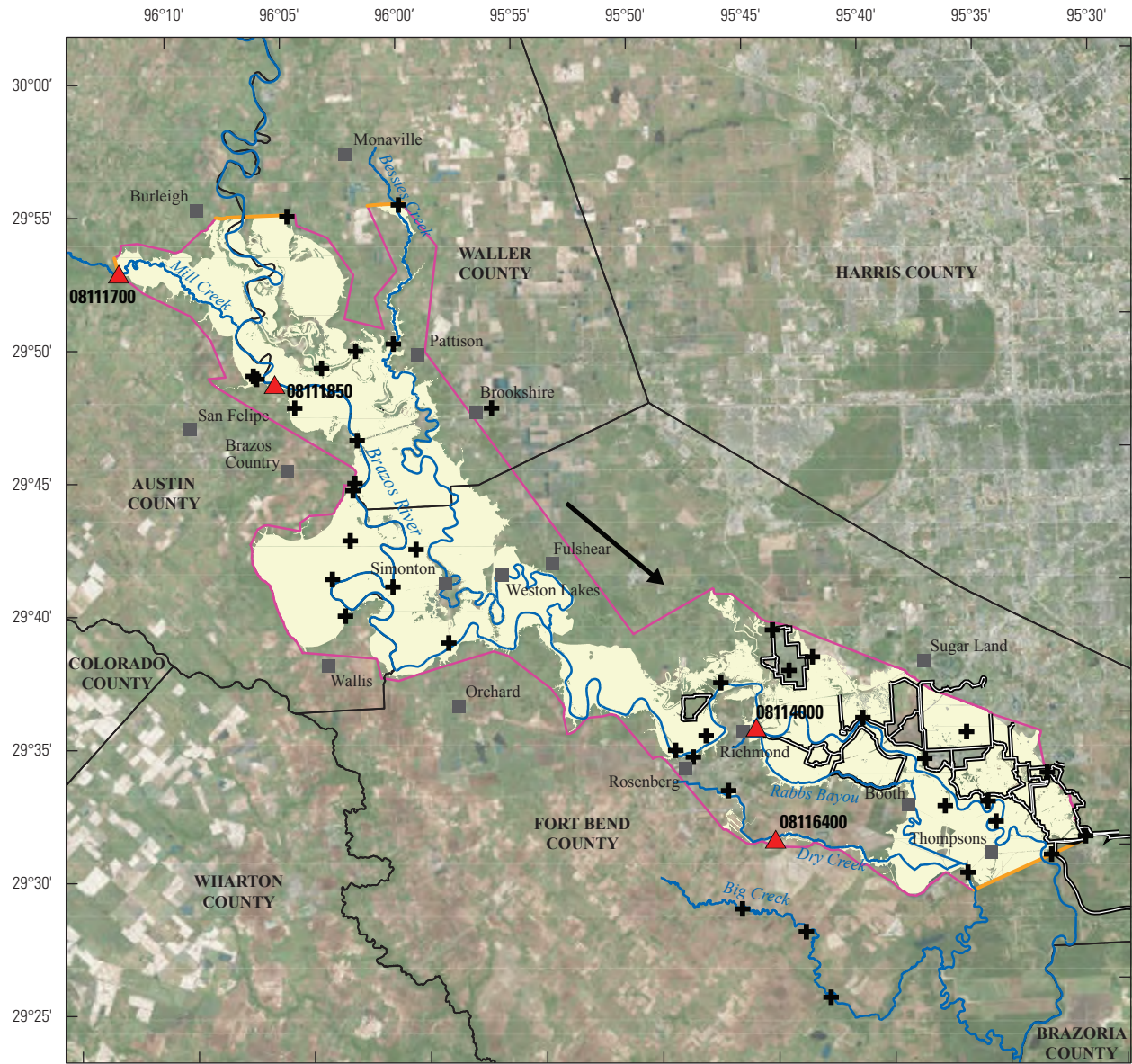
Brazos River and Tributaries

The Brazos River is the third longest river in Texas, and it flows from the headwaters in Curry County, New Mexico, to the Gulf of Mexico near Freeport, Tex. Two flood-inundation maps were created to show the areal extent of flooding in the Brazos Basin—one flood-inundation map for the upper reach and a second flood-inundation map for the lower reach (figs. 4–5).

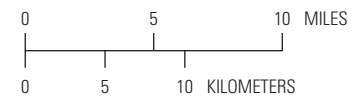
The upper reach inundation map includes 99 mi of the main stem of the Brazos River from Burleigh, Tex., downstream to Thompsons, Tex. (fig. 4). This map also includes a 43-mi reach of Bessies Creek beginning upstream from Pattison, Tex., to the confluence with the Brazos River near Fulshear, Tex., and a 9-mi reach of Mill Creek from USGS streamflow-gaging station 08111700 Mill Creek near Bellville, Tex., to the confluence with the Brazos River. Communities along the upper reach of the Brazos River include San Felipe, Wallis, Brazos Country, Simonton, Weston Lakes, Rosenberg, Richmond, Sugar Land, and Booth, Tex., covering parts of Waller, Austin, and Fort Bend Counties.

The lower reach inundation map is for a 20-mi reach of the main stem of the Brazos River from Holiday Lakes, Tex., to just upstream from Lake Jackson, Tex. (fig. 5). Communities along the lower reach include West Columbia, East Columbia, Bailey’s Prairie, Brazoria, and Lake Jackson, Tex., in Brazoria County.

A total of 46 surveyed HWMs were used to create the inundation maps for the Brazos Basin. The measured depths of water at the HWMs ranged from 0 to 8.6 ft above ground, and peak water-surface elevations ranged from 19.6 to 283.9 ft above NAVD 88. The measured depths of water at the HWMs and the surveyed peak water-surface elevation data are available for download at <https://doi.org/10.5066/F7VH5N3N> (Watson and others, 2018).



Base modified from U.S. Geological Survey digital data
 Hydrography and inundated area 1:24,000 scale
 Imagery from: Esri World Image Service
 Albers Equal Area Projection, Texas Centric Mapping System
 North American Datum of 1983 (2011)



EXPLANATION








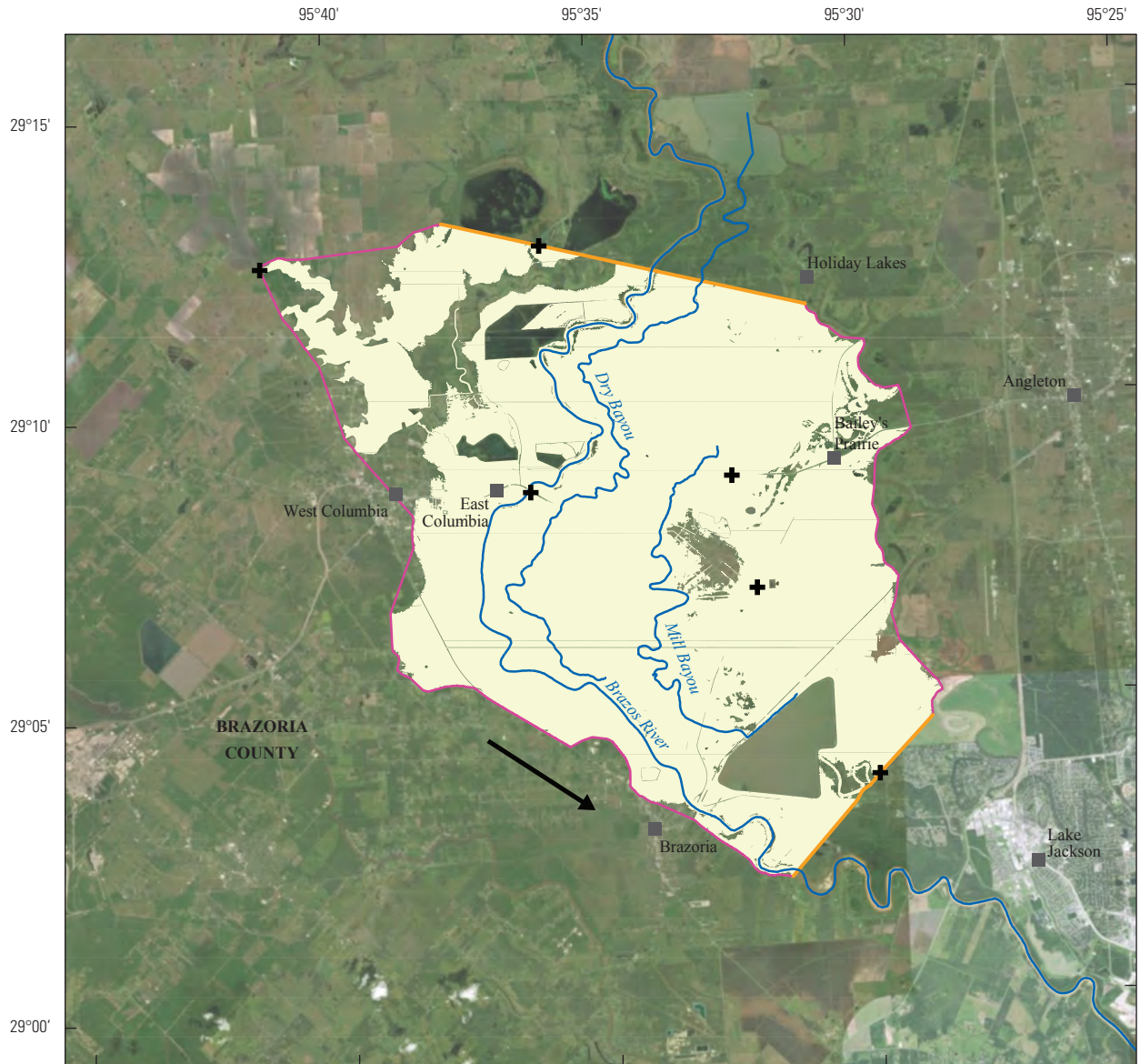
- | | | | |
|---|---|---|---|
|  | Inundated area, derived from high-water mark water-surface elevation and streamflow-gaging station data |  | Levee |
|  | Mapped boundary |  | High-water mark |
|  | Flow direction |  | U.S. Geological Survey streamflow-gaging station and number |
|  | Mapped area boundary—Restricted by high-water mark coverage | 08114000 | |

Figure 4. Flood-inundation map of the upper reach of the Brazos River for the August and September 2017 Hurricane Harvey-related flood event in southeastern Texas and southwestern Louisiana.



Base modified from U.S. Geological Survey digital data
 Hydrography and inundated area 1:24,000 scale
 Imagery from: Esri World Image Service
 Albers Equal Area Projection, Texas Centric Mapping System
 North American Datum of 1983 (2011)



EXPLANATION

- Inundated area, derived from high-water mark water-surface elevation and streamflow-gaging station data
- Mapped boundary
- Flow direction
- Mapped area boundary—Restricted by high-water mark coverage
- + High-water mark

Figure 5. Flood-inundation map of the lower reach of the Brazos River for the August and September 2017 Hurricane Harvey-related flood event in southeastern Texas and southwestern Louisiana.

The USGS operates five streamflow-gaging stations on the Brazos River and surrounding tributaries that were used in the creation of the inundation maps. The following streamflow-gaging stations were used in the creation of the maps:

1. Mill Creek near Bellville, Tex. (USGS 08111700): A peak stage of 22.49 ft above streamflow-gaging station (streamgage) datum (water-surface elevation of 145.31 ft above the National Geodetic Vertical Datum of 1929 [NGVD 29]) was recorded on August 28, 2017;
2. Brazos River at San Felipe, Tex. (USGS 08111850): A peak stage of 129.00 ft above streamgage datum (water-surface elevation of 129.00 ft above NAVD 88) was recorded on August 29, 2017;
3. Brazos River at Richmond, Tex. (USGS 08114000): A peak stage of 55.19 ft above streamgage datum (water-surface elevation of 83.13 ft above NGVD 29) was recorded on September 1, 2017;
4. Dry Creek near Rosenberg, Tex. (USGS 08116400): A peak stage of 82.53 ft above streamgage datum (water-surface elevation of 82.53 ft above NAVD 88) was recorded on August 27, 2017; and
5. Brazos River near Rosharon, Tex. (USGS 08116650): A peak stage of 52.65 ft above streamgage datum (water-surface elevation of 52.65 ft above NGVD 29) was recorded on August 29, 2017. Note that this station does not appear on figures 4 or 5 because it is located between the two mapped areas and outside of the extents of the two maps, but the peak-stage data were used to create the water-surface elevation.

Rainfall totals ranged from about 13 to 39 in. within the Brazos Basin for the duration of the event. The highest rainfall totals from this one storm event in the Brazos Basin are similar to the average annual rainfall for the study area of about 45 in. (NOAA, 2014).

Neches River and Tributaries

The headwaters of the Neches River are located in northeastern Texas; the Neches River flows approximately 428 mi to Sabine Lake near the Texas-Louisiana border. Several Texas communities are located along a 131-mi reach of the Neches River in the counties of Orange, Jasper, Hardin, Jefferson, and Tyler, including Beaumont, Evadale, Port Neches, and Central Gardens, Tex. Two flood-inundation

maps were created to show the areal extent of flooding in this 131-mi reach of the Neches Basin—one flood-inundation map for the upper reach and a second flood-inundation map for the lower reach (figs. 6–7). The upper reach of the Neches River extends from near the confluence with the Angelina River to the confluence with Black Creek (fig. 6). The lower reach of the Neches River extends from the confluence with Black Creek to Sabine Lake (fig. 7).

A total of 33 surveyed HWMs were used to create the flood-inundation maps for the Neches Basin. The measured depths of water at the HWMs ranged from 0 to 11.6 ft above ground, and peak water-surface elevations ranged from 9.2 to 200.2 ft above NAVD 88.

The USGS operates four streamflow-gaging stations on the Neches River that were used in the analysis to create the inundation maps:

1. Neches River near Rockland, Tex. (USGS 08033500): A peak stage of 32.08 ft above streamgage datum (water-surface elevation of 120.49 ft above NGVD 29) was recorded on September 1, 2017;
2. Neches River near Town Bluff, Tex. (USGS 08040600): A peak stage of 80.70 ft above streamgage datum (water-surface elevation of 80.70 ft above NGVD 29) was recorded on August 31, 2017;
3. Neches River at Evadale, Tex. (USGS 08041000): A peak stage of 25.11 ft above streamgage datum (water-surface elevation of 33.36 ft above NGVD 29) was recorded on September 2, 2017; and
4. Neches River at Saltwater Barrier at Beaumont, Tex. (USGS 08041780): A peak stage of 21.56 ft above streamgage datum (water-surface elevation of 21.56 ft above NGVD 29) was recorded on September 1, 2017.

Rainfall totals ranged from about 18 to 52 in. within the Neches Basin for the duration of the event (NOAA, 2014).

Pine Island Bayou

Pine Island Bayou, a tributary to the Neches River, flows south and east intermittently, beginning in northern Liberty County, Tex., and continuing through Hardin and Jefferson Counties, Tex., before reaching the Neches River in Orange County. The extent of the inundation map is a 68-mi reach of Pine Island Bayou through the Texas communities of Hull, Daisetta, Sour Lake, Nome, Bevil Oaks, Rose Hill Acres, and the outskirts of Beaumont (fig. 8).

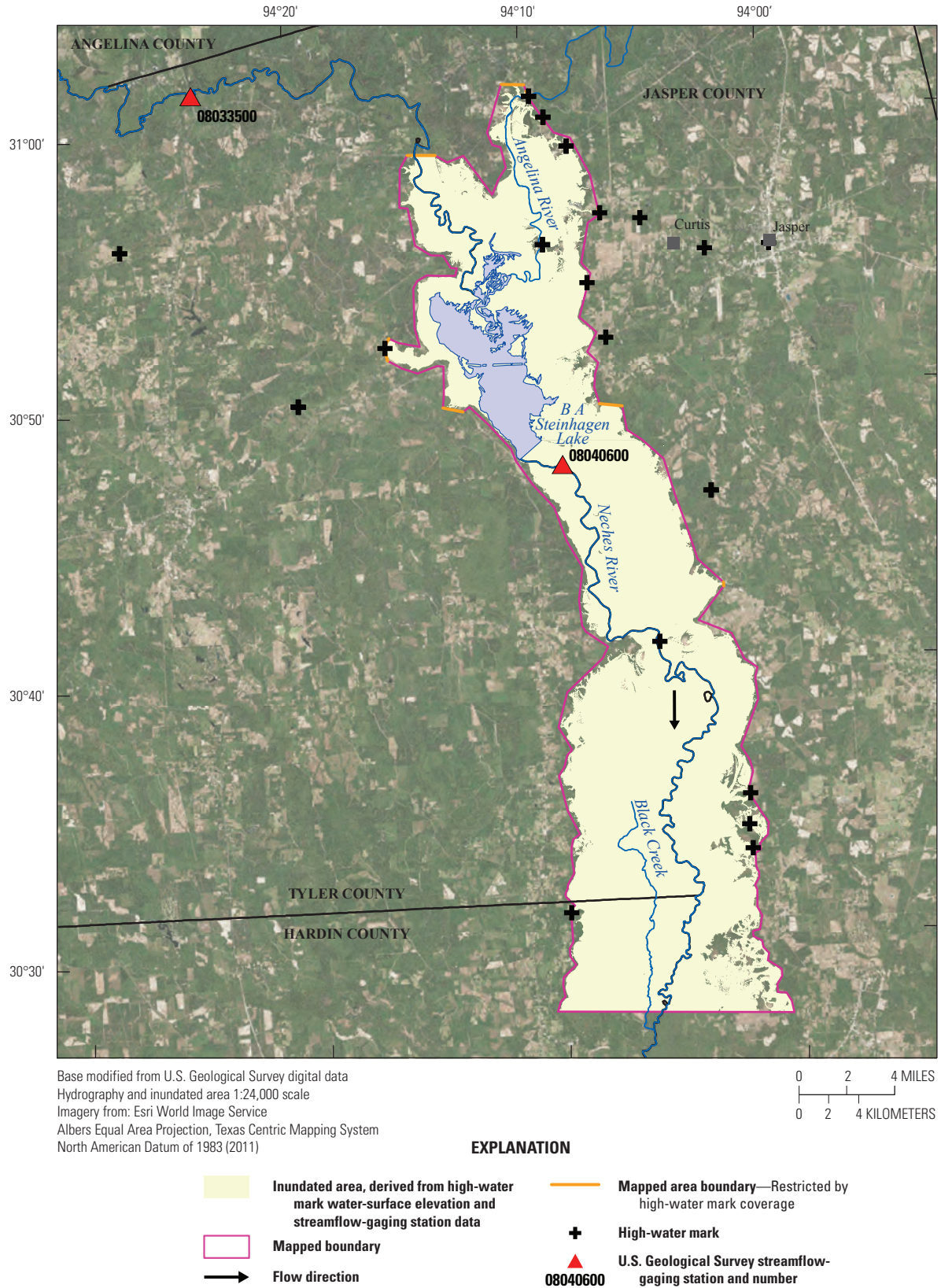
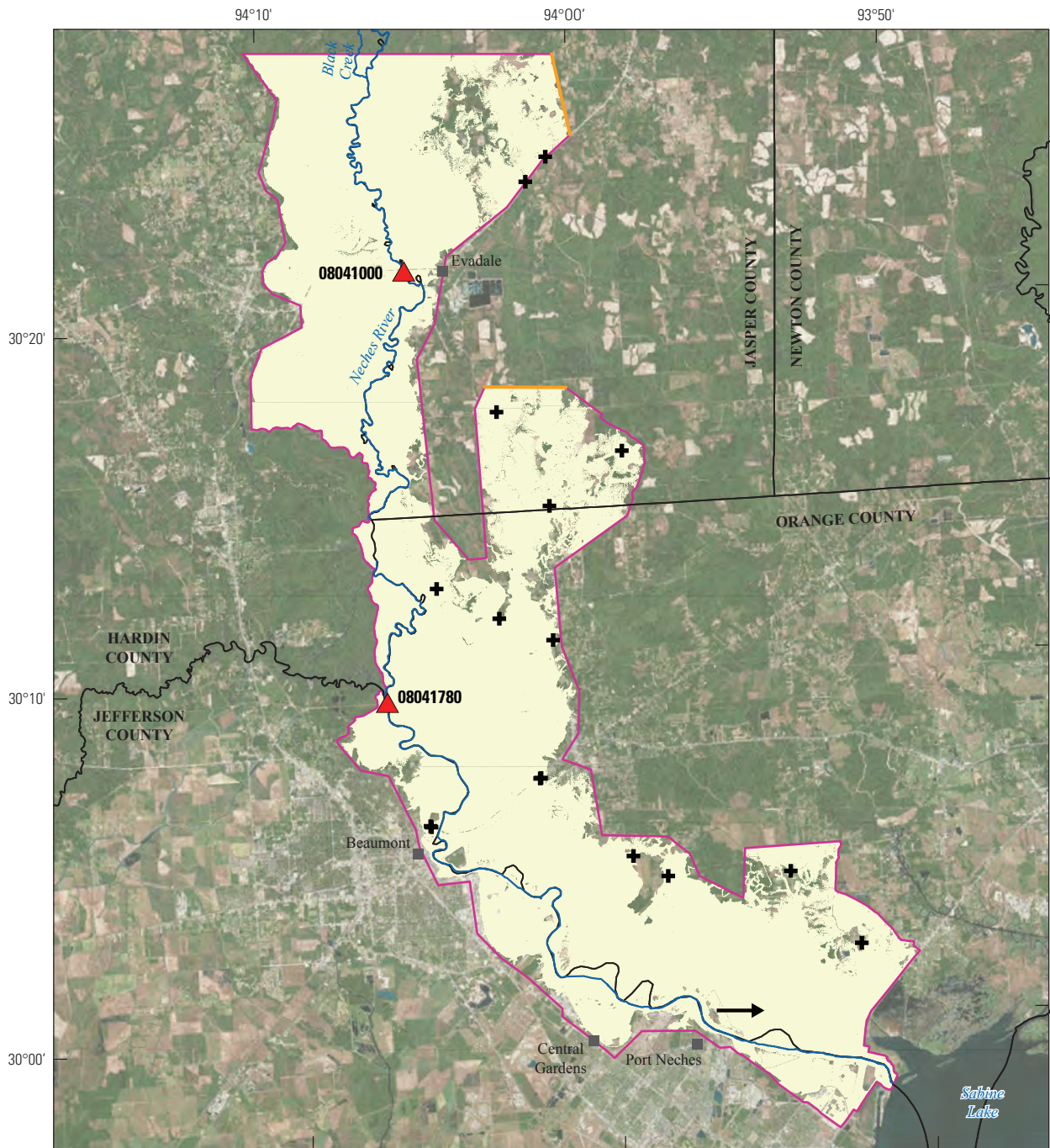


Figure 6. Flood-inundation map of the upper reach of the Neches River for the August and September 2017 Hurricane Harvey-related flood event in southeastern Texas and southwestern Louisiana.



Base modified from U.S. Geological Survey digital data
 Hydrography and inundated area 1:24,000 scale
 Imagery from: Esri World Image Service
 Albers Equal Area Projection, Texas Centric Mapping System
 North American Datum of 1983 (2011)



EXPLANATION

- | | | | |
|--|---|--|---|
| | Inundated area, derived from high-water mark water-surface elevation and streamflow-gaging station data | | Mapped area boundary—Restricted by high-water mark coverage |
| | Mapped boundary | | High-water mark |
| | Flow direction | | U.S. Geological Survey streamflow-gaging station and number |

Figure 7. Flood-inundation map of the lower reach of the Neches River for the August and September 2017 Hurricane Harvey-related flood event in southeastern Texas and southwestern Louisiana.

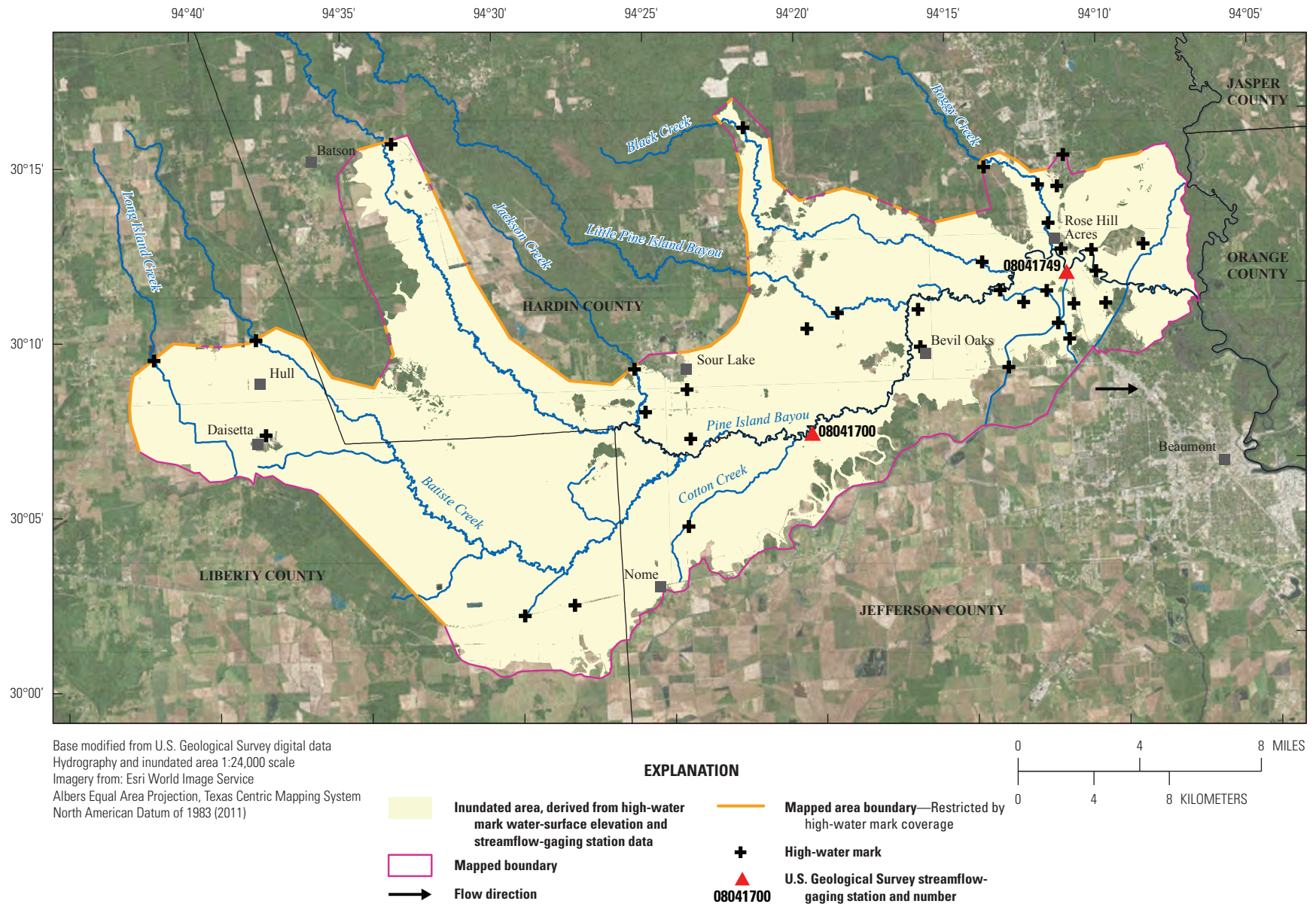


Figure 8. Flood-inundation map of Pine Island Bayou, a tributary to the Neches River, for the August and September 2017 Hurricane Harvey-related flood event in southeastern Texas and southwestern Louisiana.

A total of 34 surveyed HWMs in the Pine Island Bayou Subbasin were used in the creation of the inundation map. The measured depths of water at the HWMs ranged from 0 to 14.3 ft above ground, and the peak water-surface elevations ranged from 16.3 to 79.3 ft above NAVD 88. The USGS operates two streamflow-gaging stations on Pine Island Bayou that were used in the creation of the inundation map:

1. Pine Island Bayou near Sour Lake, Tex. (USGS 08041700): A peak stage of 39.68 ft above streamgage datum (water-surface elevation of 39.68 ft above NGVD 29) was recorded on August 30, 2017; and
2. Pine Island Bayou above BI Pump Plant, Beaumont, Tex. (USGS 08041749), was inundated during the storm event, and a HWM peak of 28.97 ft above streamgage datum (water-surface elevation of 28.13 ft above NAVD 88) were documented on October 18, 2017. The date of the peak of 28.13 ft was not recorded because the station was damaged during the storm event, but the estimated date of the peak is August 30, 2017.

Rainfall totals ranged from about 24 to 44 in. within the Pine Island Bayou Subbasin for the duration of the event. The highest rainfall totals from this one storm event in the Pine Island Bayou Subbasin are similar to the average annual rainfall for the study area of about 45 in. (NOAA, 2014).

Sabine River and Tributaries

From its headwaters in Hunt County in north Texas, the Sabine River flows approximately 510 mi to its mouth at Sabine Lake on the Texas-Louisiana border near the Gulf of Mexico. Numerous communities in Jasper, Newton, Orange, and Jefferson Counties in Texas and Beauregard, Calcasieu, and Cameron Parishes in Louisiana are located along a 131-mi reach of the Sabine River, including Newton, Tex., Bon Wier, Tex., Merryville, La., Kirbyville, Tex., Buna, Tex., Deweyville, Tex., Starks, La., Mauriceville, Tex., Vidor, Tex., Orange, Tex., West Orange, Tex., Pinehurst, Tex., and Bridge City, Tex. Separate flood-inundation maps were created to show the areal extent of flooding in the Sabine Basin in the upper, middle, and lower reaches of the Sabine River (figs. 9–11).

A total of 70 HWMs were surveyed and used to make flood-inundation maps for the Sabine Basin. Of these 70 HWMs, 43 were used to make separate flood-inundation maps for either the upper, middle, or lower reaches of the Sabine River—13 HWMs in the upper reach, 12 HWMs in the middle reach, and 18 HWMs in the lower reach. The remaining 27 HWMs were used to make flood-inundation maps for tributaries to the Sabine River. For all 70 HWMs in the Sabine Basin, the measured depths of water at the HWMs

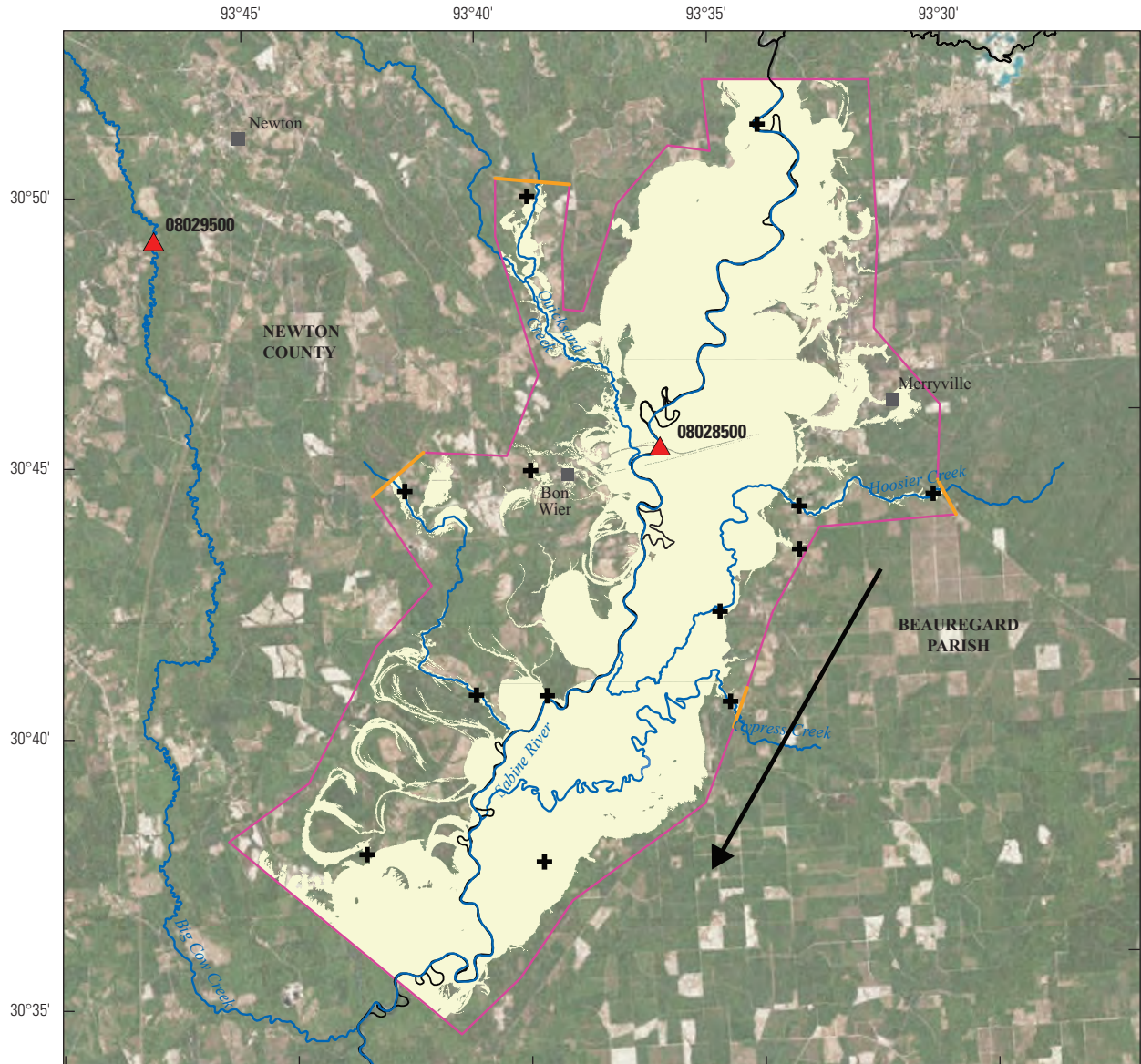
ranged from 0 to 7.0 ft above ground, and the peak water-surface elevations associated with the HWMs ranged from 5.7 to 117.5 ft above NAVD 88.

The USGS operates four streamflow-gaging stations on the Sabine River that were used to create flood-inundation maps for the Sabine Basin. One tributary station, Cow Bayou near Mauriceville, Tex. (USGS 08031000), was damaged during the storm event and not used in the creation of the inundation maps. The following streamflow-gaging stations were used in the creation of the Sabine Basin flood-inundation maps:

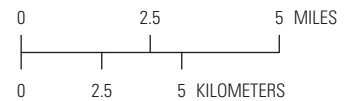
1. Sabine River near Bon Wier, Tex. (USGS 08028500): A peak stage of 38.93 ft above streamgage datum (water-surface elevation of 72.35 ft above NGVD 29) was recorded on September 2, 2017;
2. Big Cow Creek near Newton, Tex. (USGS 08029500): A peak stage of 21.08 ft above streamgage datum (water-surface elevation of 155.77 ft above NGVD 29) was recorded on August 30, 2017;
3. Sabine River near Ruliff, Tex. (USGS 08030500): A peak stage of 31.60 ft above streamgage datum (water-surface elevation of 25.68 ft above NGVD 29) was recorded on September 2, 2017; and
4. Sabine River (at Navy Pier) at Orange, Tex. (USGS 08030540): A peak stage of 7.94 ft above streamgage datum (water-surface elevation of 7.94 ft above NAVD 88) was recorded on September 3, 2017.

In the upper reach of the Sabine Basin, the measured depths of water at the HWMs ranged from 0 to 6.6 ft above ground, and the peak water-surface elevations ranged from 55.7 to 117.5 ft above NAVD 88. Data from one USGS streamflow-gaging station (Sabine River near Bon Wier, Tex.) were used to help create the inundation map for the upper reach (fig. 9). In the middle reach of the Sabine Basin, the measured depths of water at the HWMs ranged from 0 to 7.0 ft above ground, and the peak water-surface elevations ranged from 32.0 to 116.2 ft above NAVD 88. In the lower reach of the Sabine Basin, the measured depths of water at the HWMs ranged from 0 to 7.0 ft above ground, and the peak water-surface elevations ranged from 5.7 to 24.4 ft above NAVD 88. Data from two USGS streamflow-gaging stations were used for the inundation analysis for the lower reach: Sabine River near Ruliff, Tex., and Sabine River (at Navy Pier) at Orange, Tex.

Rainfall totals ranged from about 19 to 48 in. within the Sabine Basin over the duration of the event. The highest rainfall totals from this one storm event in the Sabine Basin exceed the average annual rainfall for the area of about 45 in. (NOAA, 2014).



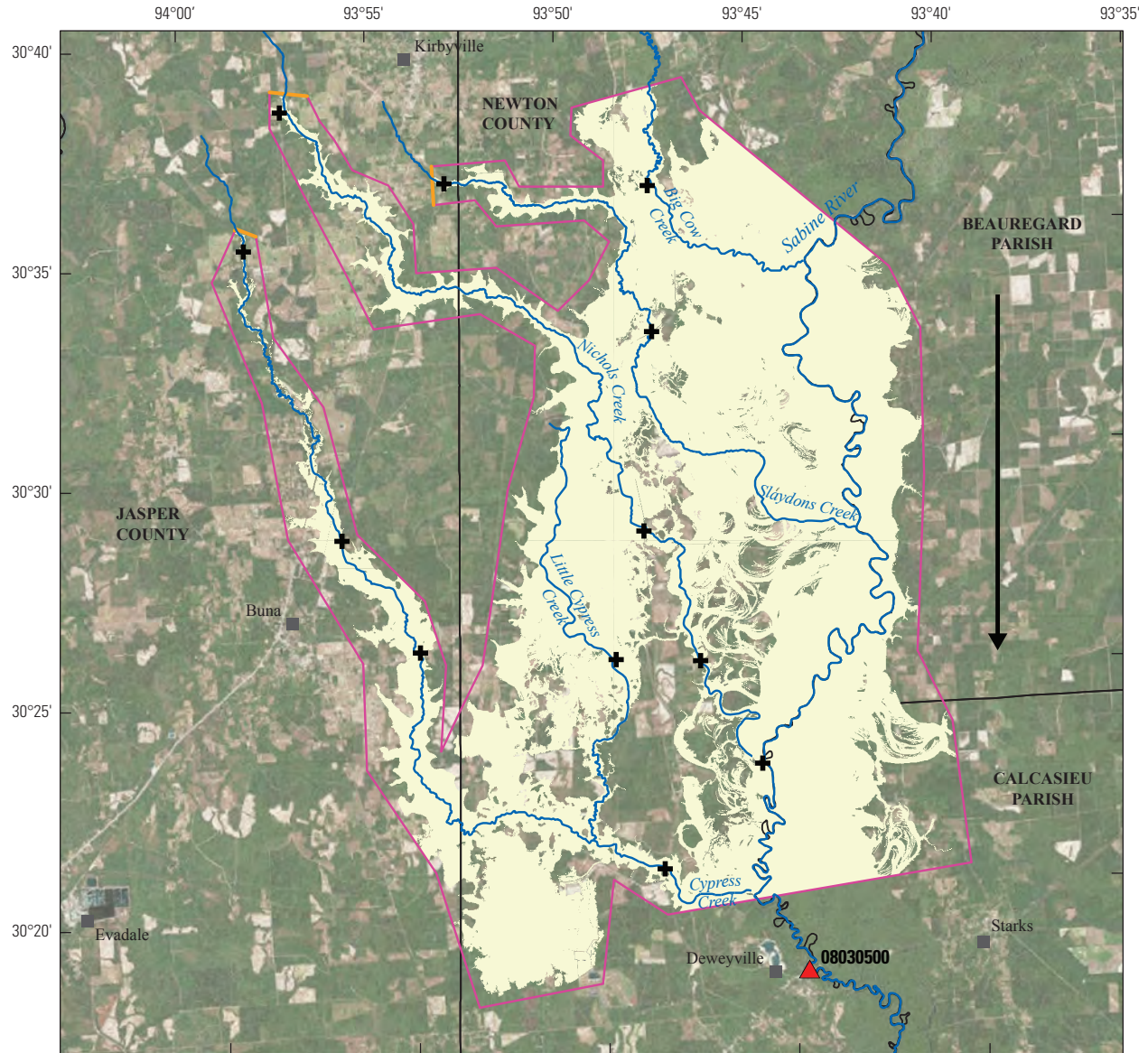
Base modified from U.S. Geological Survey digital data
 Hydrography and inundated area 1:24,000 scale
 Imagery from: Esri World Image Service
 Albers Equal Area Projection, Texas Centric Mapping System
 North American Datum of 1983 (2011)



EXPLANATION

- Inundated area, derived from high-water mark water-surface elevation and streamflow-gaging station data
- Mapped boundary
- Flow direction
- Mapped area boundary—Restricted by high-water mark coverage
- + High-water mark
- ▲ U.S. Geological Survey streamflow-gaging station and number

Figure 9. Flood-inundation map of the upper reach of the Sabine River for the August and September 2017 Hurricane Harvey-related flood event in southeastern Texas and southwestern Louisiana.



Base modified from U.S. Geological Survey digital data
 Hydrography and inundated area 1:24,000 scale
 Imagery from: Esri World Image Service
 Albers Equal Area Projection, Texas Centric Mapping System
 North American Datum of 1983 (2011)

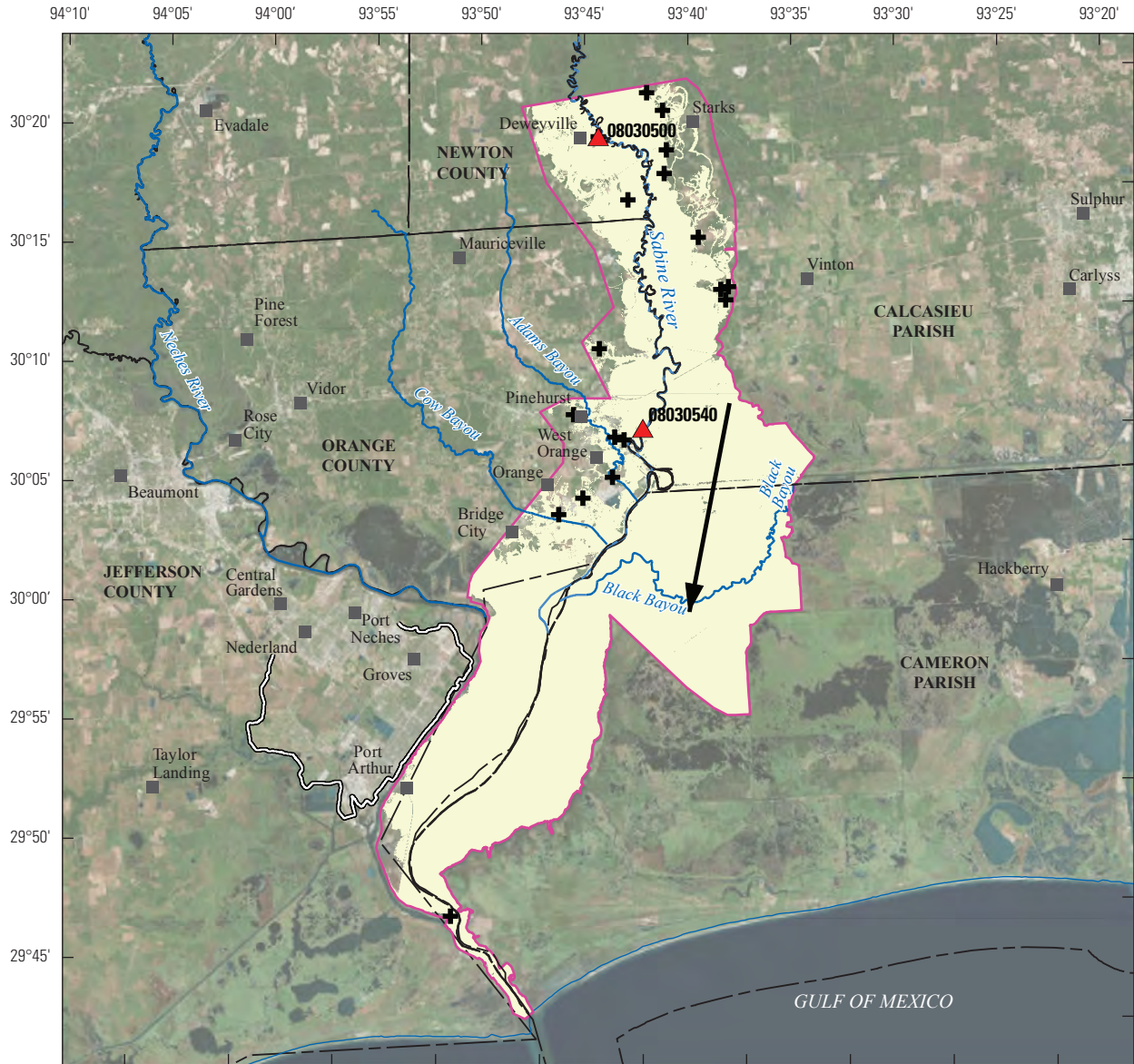


EXPLANATION

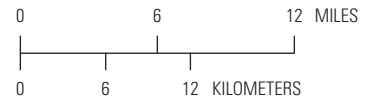
- Inundated area, derived from high-water mark water-surface elevation and streamflow-gaging station data
- Mapped boundary
- Flow direction
- Mapped area boundary—Restricted by high-water mark coverage
- + High-water mark
- U.S. Geological Survey streamflow-gaging station and number
08030500

Figure 10. Flood-inundation map of the middle reach of the Sabine River for the August and September 2017 Hurricane Harvey-related flood event in southeastern Texas and southwestern Louisiana.

26 Characterization of Peak Streamflows and Flood Inundations from Hurricane Harvey, 2017



Base modified from U.S. Geological Survey digital data
 Hydrography and inundated area 1:24,000 scale
 Imagery from: Esri World Image Service
 Albers Equal Area Projection, Texas Centric Mapping System
 North American Datum of 1983 (2011)



EXPLANATION

- Inundated area, derived from high-water mark water-surface elevation and streamflow-gaging station data
- Mapped boundary
- Flow direction
- Levee
- + High-water mark
- ▲ U.S. Geological Survey streamflow-gaging station and number
08030540

Figure 11. Flood-inundation map of the lower reach of the Sabine River for the August and September 2017 Hurricane Harvey-related flood event in southeastern Texas and southwestern Louisiana.

Big Cow Creek

Big Cow Creek, a tributary to the Sabine River, flows south towards the Sabine River near Newton and Kirbyville, Tex., in Jasper and Newton Counties. The extent of the inundation map is a 37-mi reach of Big Cow Creek and its tributary, Trout Creek (fig. 12). Eight HWMs were surveyed in the Big Cow Creek Basin and used to make the inundation map for the area near Kirbyville, Tex., and surrounding areas. The measured depths of water at these eight HWMs ranged from 1.8 to 6.2 ft above ground, and the peak water-surface elevations ranged from 95.4 to 265.9 ft above NAVD 88. Data from one USGS streamflow-gaging station were also used to make the Big Cow Creek inundation map: Big Cow Creek near Newton, Tex. (USGS 08029500), where a peak stage of 21.08 ft above streamgage datum (water-surface elevation of 155.77 ft above NGVD 29) was recorded on August 30, 2017.

Cow Bayou

Cow Bayou, a tributary to the Sabine River, flows south toward Bridge City, Tex., near Mauriceville, Tex., in Jasper, Newton, and Orange Counties. The extent of the inundation map is a 23-mi reach of Cow Bayou from its headwaters northeast of Evadale, Tex., to State Highway 87 at Bridge City near the Sabine River (fig. 13). A total of 19 surveyed HWMs in the Cow Bayou Basin were used to make the inundation map in the community of Mauriceville and surrounding areas. The measured depths of water at the HWMs ranged from 0 to 6.2 ft above ground, and the peak water-surface elevations ranged from 7.6 to 55.5 ft above NAVD 88. One USGS streamflow-gaging station within the Cow Bayou Basin, Cow Bayou near Mauriceville, Tex. (USGS 08031000), was damaged during the storm event, so data from this streamflow-gaging station were not available to help make the flood-inundation map for Cow Bayou.

San Bernard River

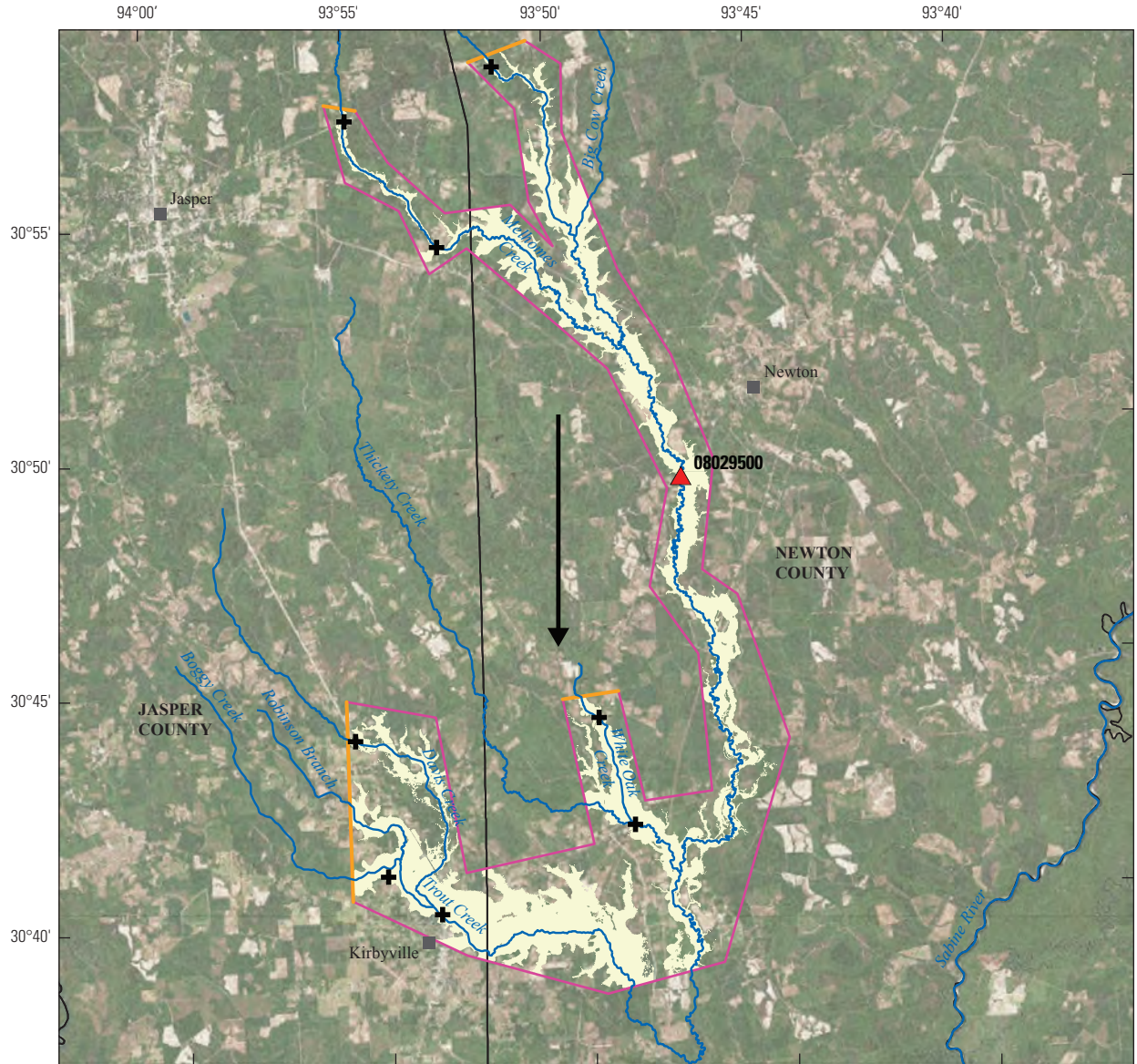
The San Bernard River generally flows southeast through Texas from the headwaters near New Ulm, Tex., to its mouth

on the Gulf of Mexico. Separate inundation maps were created to show the areal extent of flooding in the San Bernard Coastal Basin in the upper, middle, and lower reaches of the river (figs. 14–16). The upper reach includes 20 mi of the San Bernard River, extending from northwest of Interstate 10 near Sealy, Tex., on the upstream end and continuing downstream through the Attwater Prairie National Wildlife Refuge in Colorado County, Tex. (fig. 14). The middle reach includes 46 mi of the San Bernard River, extending from Wallis, Tex., in Austin County downstream through East Bernard, Tex., in Wharton County and Kendleton, Tex., in Fort Bend County (fig. 15). The lower reach includes 33 mi of the San Bernard River. In this reach, the San Bernard River flows past Sweeny and Brazoria, Tex., in Brazoria County; the downstream extent terminates at the San Bernard National Wildlife Refuge (fig. 16).

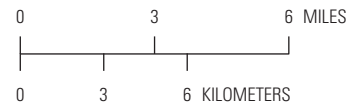
A total of 34 HWMs surveyed along the San Bernard River were used to create flood-inundation maps: 7 HWMs in the upper reach, 17 HWMs in the middle reach, and 10 HWMs in the lower reach. The measured depths of water at the HWMs ranged from 0 to 6.8 ft above ground, and the peak water-surface elevations ranged from 8.0 to 253.2 ft above NAVD 88. The USGS operates two streamflow-gaging stations on the San Bernard River that were used in the creation of the inundation maps:

1. San Bernard River near Boling, Tex. (USGS 08117500): A peak stage of 43.79 ft above streamgage datum (water-surface elevation of 74.60 ft above NGVD 29) was recorded on August 31, 2017; and
2. San Bernard River near Sweeny, Tex. (USGS 08117705): A peak stage of 30.16 ft above streamgage datum (water-surface elevation of 30.16 ft above NAVD 88) was recorded on September 2, 2017.

Rainfall totals ranged from about 11 to 33 in. within the San Bernard Coastal Basin over the duration of the event. The highest rainfall totals from this one storm event in the San Bernard Coastal Basin represent more than 70 percent of the average annual rainfall for the area (about 45 in.) (NOAA, 2014).

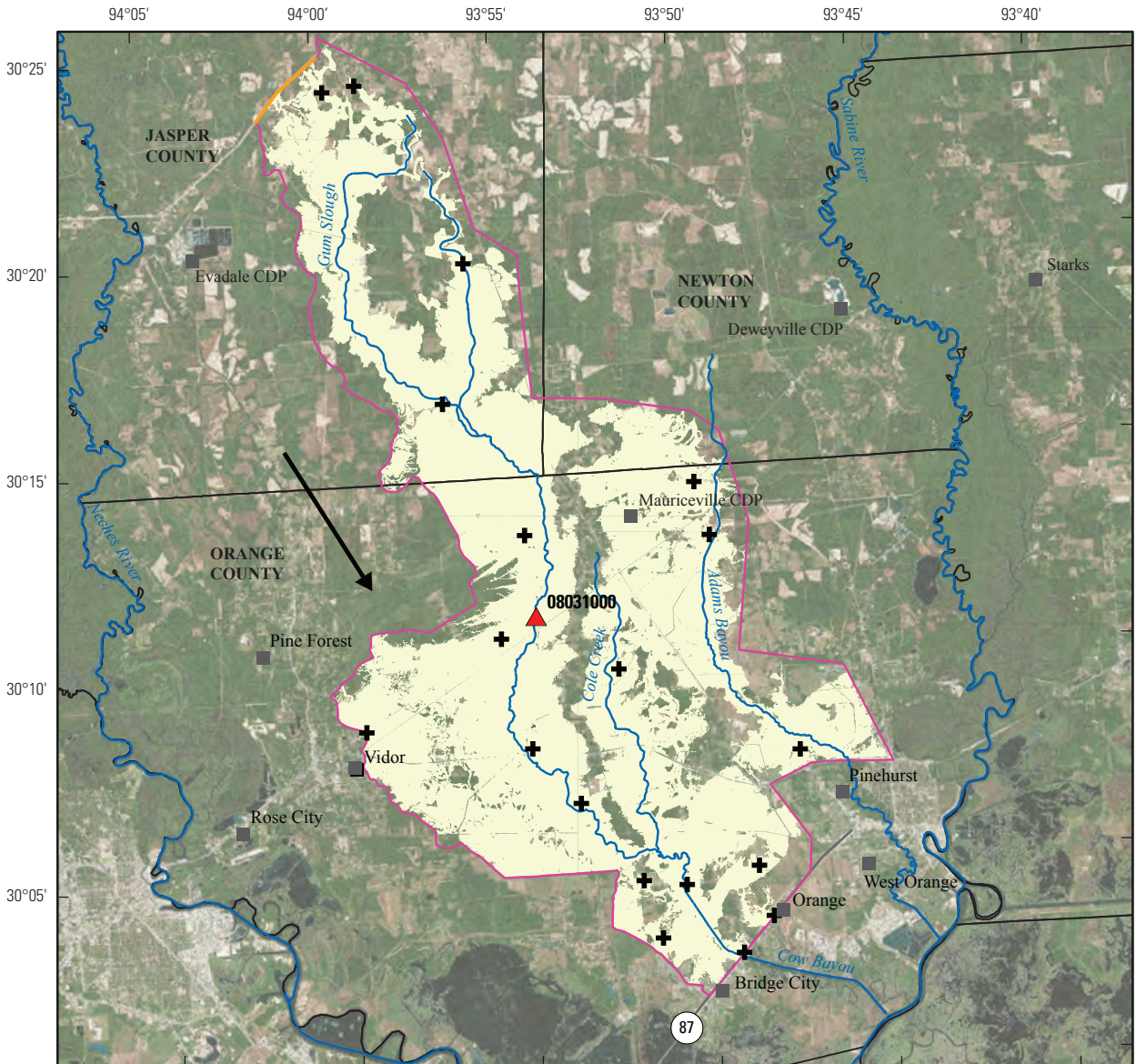


Base modified from U.S. Geological Survey digital data
 Hydrography and inundated area 1:24,000 scale
 Imagery from: Esri World Image Service
 Albers Equal Area Projection, Texas Centric Mapping System
 North American Datum of 1983 (2011)

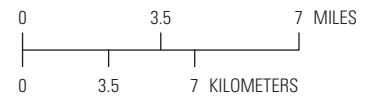


- EXPLANATION**
- Inundated area, derived from high-water mark water-surface elevation and streamflow-gaging station data
 - Mapped boundary
 - Flow direction
 - Mapped area boundary—Restricted by high-water mark coverage
 - + High-water mark
 - ▲ U.S. Geological Survey streamflow-gaging station and number
08029500

Figure 12. Flood-inundation map of Big Cow Creek, a tributary to the Sabine River, for the August and September 2017 Hurricane Harvey-related flood event in southeastern Texas and southwestern Louisiana.



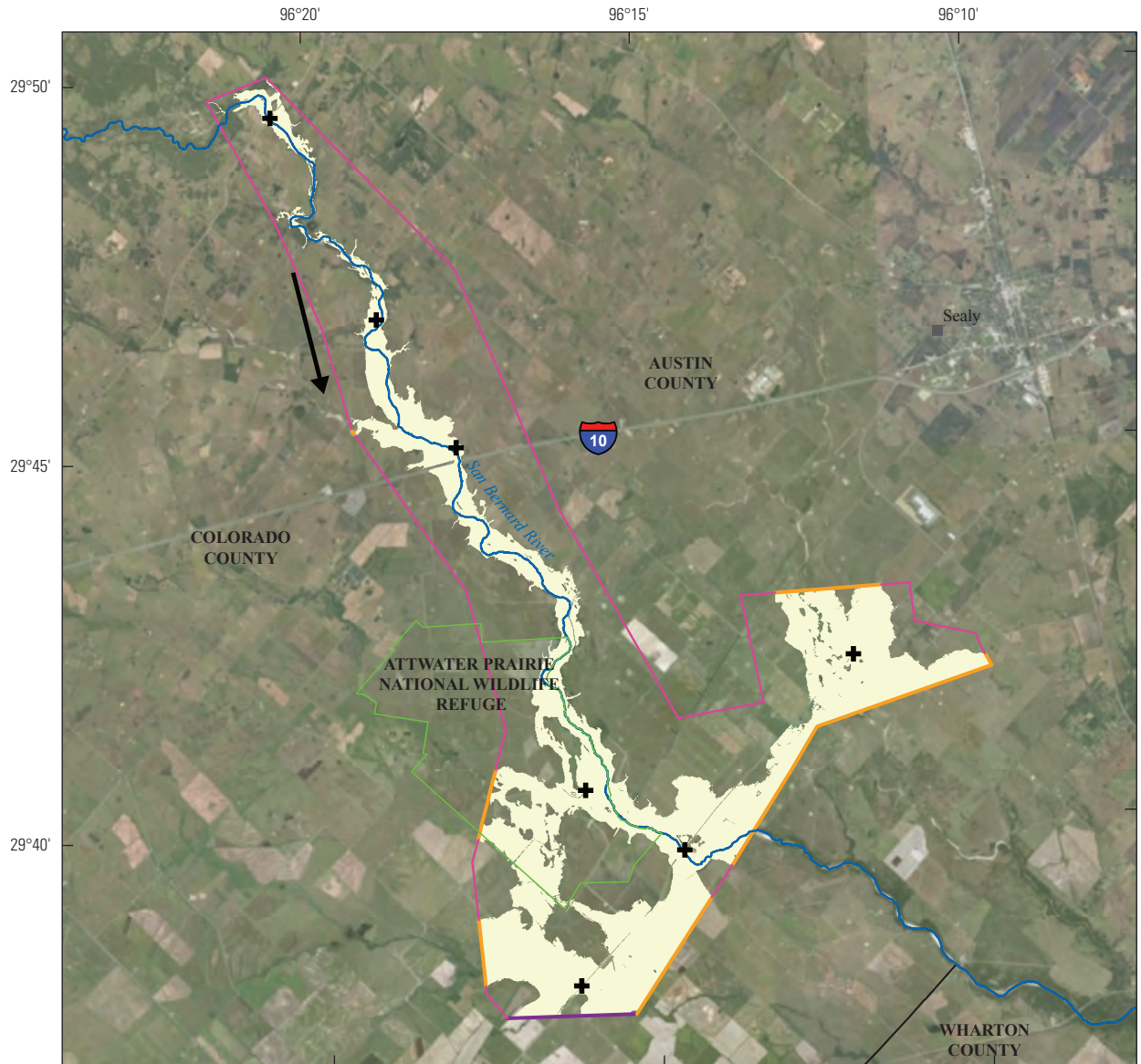
Base modified from U.S. Geological Survey digital data
 Hydrography and inundated area 1:24,000 scale
 Imagery from: Esri World Image Service
 Albers Equal Area Projection, Texas Centric Mapping System
 North American Datum of 1983 (2011)



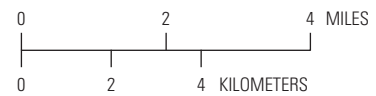
EXPLANATION

- Inundated area, derived from high-water mark water-surface elevation and streamflow-gaging station data
- Mapped boundary
- Flow direction
- Mapped area boundary—Restricted by high-water mark coverage
- + High-water mark
- ▲ U.S. Geological Survey streamflow-gaging station and number
08031000

Figure 13. Flood-inundation map of Cow Bayou, a tributary to the Sabine River, for the August and September 2017 Hurricane Harvey-related flood event in southeastern Texas and southwestern Louisiana.



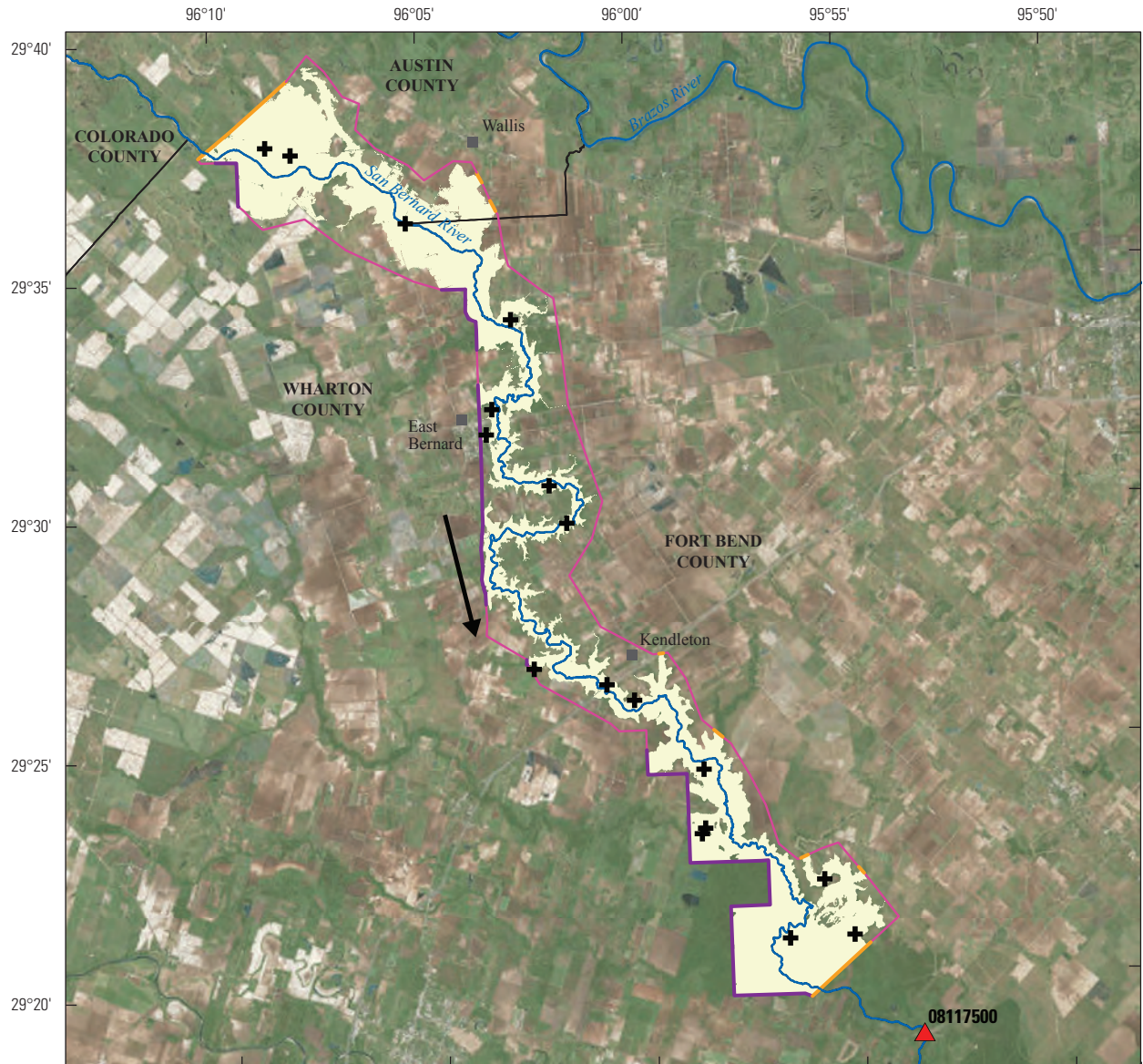
Base modified from U.S. Geological Survey digital data
 Hydrography and inundated area 1:24,000 scale
 Imagery from: Esri World Image Service
 Albers Equal Area Projection, Texas Centric Mapping System
 North American Datum of 1983 (2011)



EXPLANATION

- Inundated area, derived from high-water mark water-surface elevation and streamflow-gaging station data
- Mapped boundary
- Flow direction
- Mapped area boundary—Restricted by high-water mark coverage
- Mapped area boundary—Restricted by lack of ground surface elevation data
- High-water mark

Figure 14. Flood-inundation map of the upper reach of the San Bernard River for the August and September 2017 Hurricane Harvey-related flood event in southeastern Texas and southwestern Louisiana.

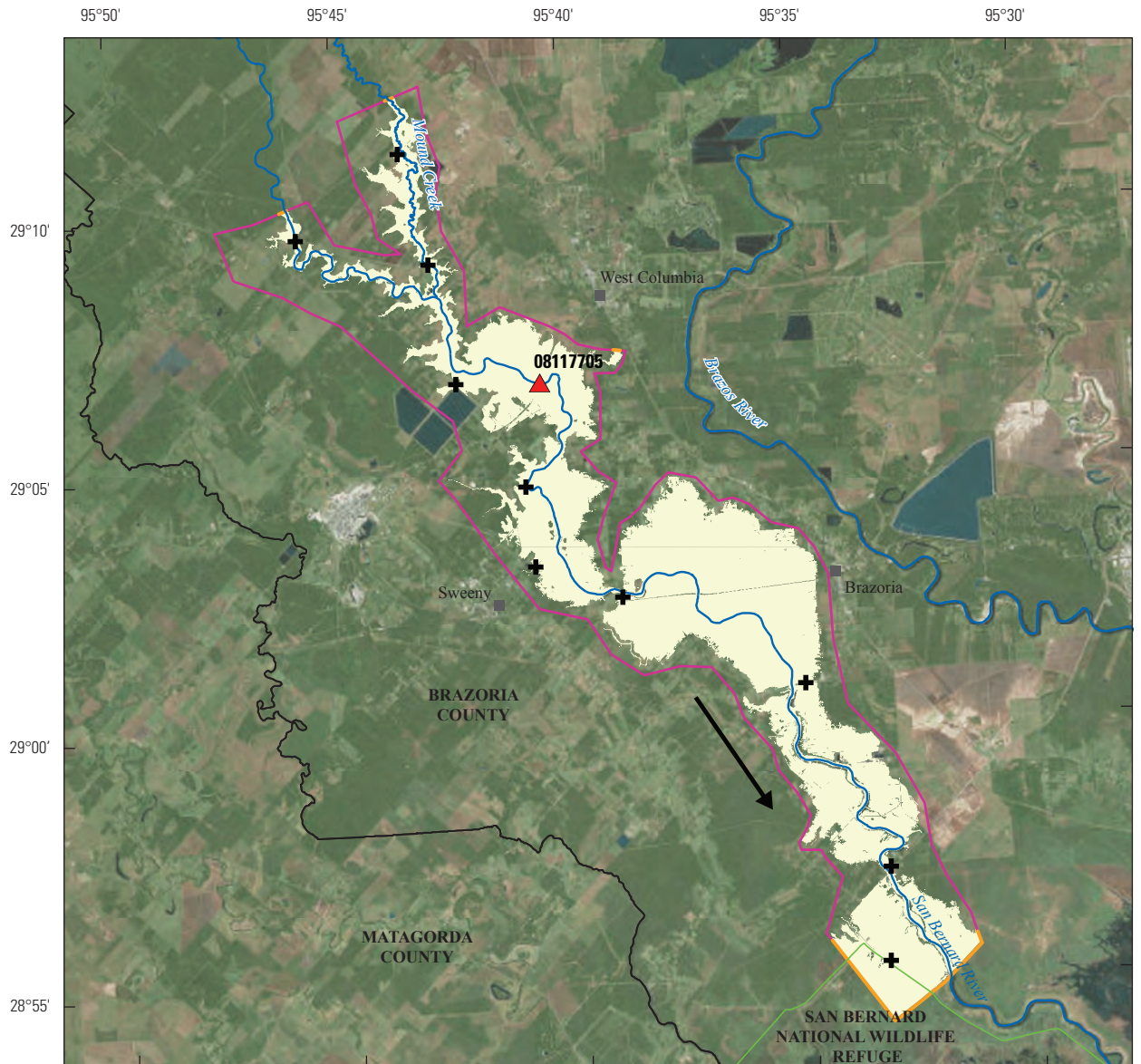


Base modified from U.S. Geological Survey digital data
 Hydrography and inundated area 1:24,000 scale
 Imagery from: Esri World Image Service
 Albers Equal Area Projection, Texas Centric Mapping System
 North American Datum of 1983 (2011)

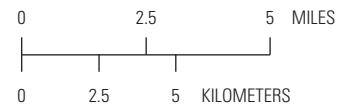


- EXPLANATION**
- Inundated area, derived from high-water mark water-surface elevation and streamflow-gaging station data
 - Mapped boundary
 - Flow direction
 - Mapped area boundary—Restricted by high-water mark coverage
 - Mapped area boundary—Restricted by lack of ground surface elevation data
 - + High-water mark
 - ▲ U.S. Geological Survey streamflow-gaging station and number
08117500

Figure 15. Flood-inundation map of the middle reach of the San Bernard River for the August and September 2017 Hurricane Harvey-related flood event in southeastern Texas and southwestern Louisiana.



Base modified from U.S. Geological Survey digital data
 Hydrography and inundated area 1:24,000 scale
 Imagery from: Esri World Image Service
 Albers Equal Area Projection, Texas Centric Mapping System
 North American Datum of 1983 (2011)



EXPLANATION

- Inundated area, derived from high-water mark water-surface elevation and streamflow-gaging station data
- Mapped boundary
- Flow direction
- Mapped area boundary—Restricted by high-water mark coverage
- High-water mark
- U.S. Geological Survey streamflow-gaging station and number
08117705

Figure 16. Flood-inundation map of the lower reach of the San Bernard River for the August and September 2017 Hurricane Harvey-related flood event in southeastern Texas and southwestern Louisiana.

San Jacinto River and Tributaries

The San Jacinto River flows south-southeast from its headwaters in Grimes and Walker Counties in Texas to Galveston Bay and includes the West Fork San Jacinto River and the East Fork San Jacinto River. The inundation map of the West Fork San Jacinto River is a 36-mi reach of the main stem of the San Jacinto River near Conroe, Tex., and includes Cypress Creek (53-mi reach), Little Cypress Creek (21-mi reach), Willow Creek (6-mi reach), Spring Creek (68-mi reach), Walnut Creek (15-mi reach), Panther Branch (11-mi reach), Lake Creek (7-mi reach), and Crystal Creek (2-mi reach) (fig. 17). The inundation map of the East Fork San Jacinto River is a 65-mi reach of the main stem of the San Jacinto River near Magnolia, Tex., and includes White Oak Creek (9-mi reach), Caney Creek (31-mi reach), Peach Creek (19-mi reach), Winters Bayou (33-mi reach), and Luce Bayou (9-mi reach) (fig. 18). The 18-mi reach of the San Jacinto River from the confluence of the West and East Forks to the Lake Houston Dam near Kingwood, Tex., is also included in the inundation map (fig. 18).

A total of 106 surveyed HWMs in the entire San Jacinto Basin were used in the creation of the two inundation maps. The measured depths of water at the HWMs ranged from 0 to 9.6 ft above ground, and peak water-surface elevations ranged from 52.3 to 276.4 ft above NAVD 88.

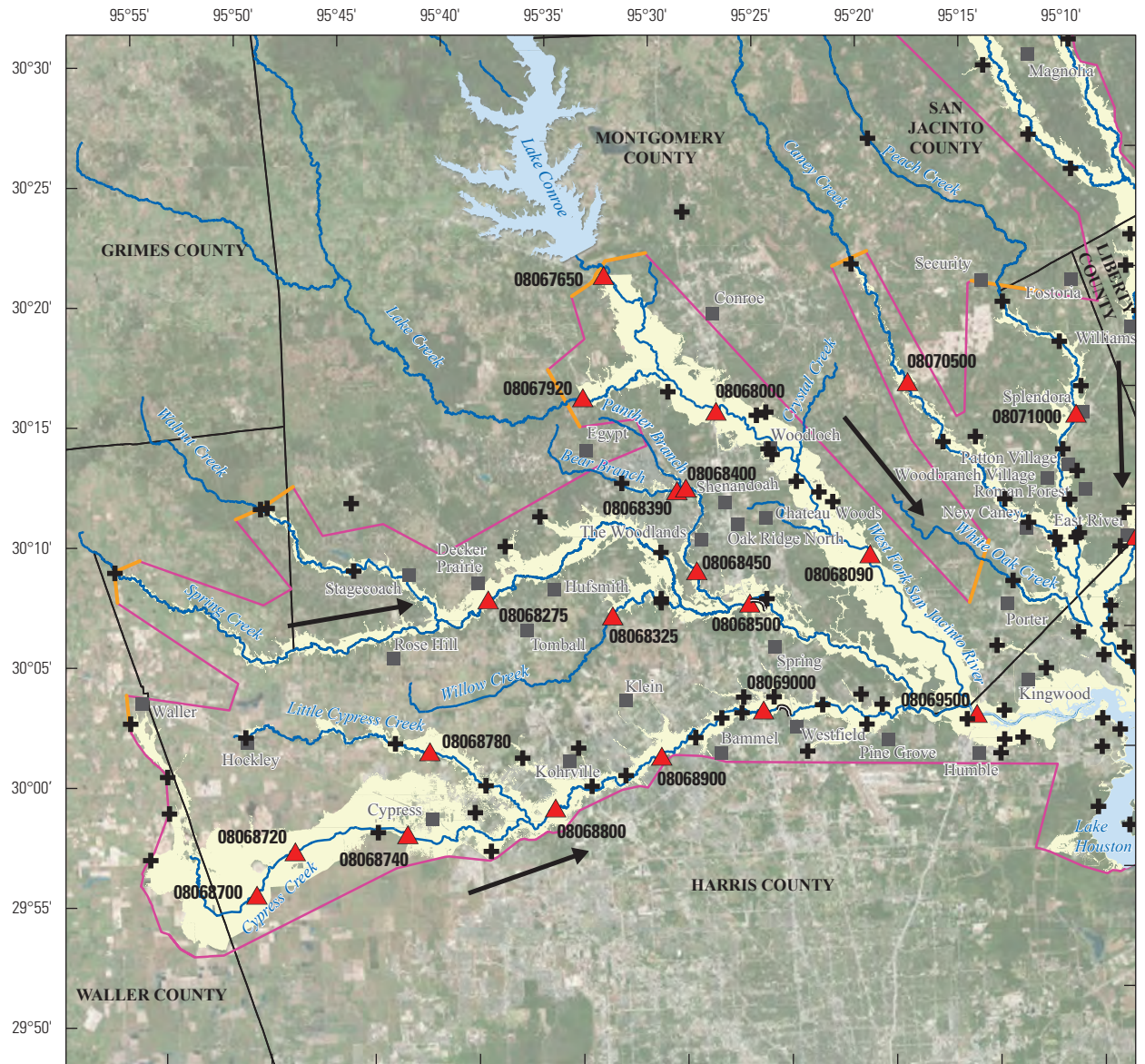
The USGS operates 22 streamflow-gaging stations on the San Jacinto River and its tributaries that were used in the creation of the inundation maps:

1. Cypress Creek at Sharp Road near Hockley, Tex. (USGS 08068700): A peak stage of 170.05 ft above streamgage datum (water-surface elevation of 170.05 ft above NAVD 88) was recorded on August 28, 2017;
2. Cypress Creek at Katy-Hockley Road near Hockley, Tex. (USGS 08068720): A peak stage of 162.85 ft above streamgage datum (water-surface elevation of 162.85 ft above NAVD 88) was recorded on August 28, 2017;
3. Cypress Creek at House-Hahl Road near Cypress, Tex. (USGS 08068740): A peak stage of 149.30 ft above streamgage datum (water-surface elevation of 149.30 ft above NAVD 88) was recorded on August 28, 2017;
4. Little Cypress Creek near Cypress, Tex. (USGS 08068780): A peak stage of 161.23 ft above streamgage datum (water-surface elevation of 161.23 ft above NAVD 88) was recorded on August 28, 2017;
5. Cypress Creek at Grant Road near Cypress, Tex. (USGS 08068800): A peak stage of 129.97 ft above streamgage datum (water-surface elevation of 129.97 ft above NAVD 88) was recorded on August 28, 2017;
6. Cypress Creek at Stuebner-Airline Road near Westfield, Tex. (USGS 08068900): A peak stage of 113.82 ft above streamgage datum (water-surface elevation of 113.82 ft above NAVD 88) was recorded on August 28, 2017;
7. Cypress Creek near Westfield, Tex. (USGS 08069000): A peak stage of 97.12 ft above streamgage datum (water-surface elevation of 97.12 ft above NAVD 88) was recorded on August 28, 2017;
8. West Fork San Jacinto River near Humble, Tex. (USGS 08069500): A peak stage of 69.18 ft above streamgage datum (water-surface elevation of 69.18 ft above NAVD 88) was recorded on August 29, 2017;
9. Spring Creek near Tomball, Tex. (USGS 08068275): A peak stage of 166.38 ft above streamgage datum (water-surface elevation of 166.38 ft above NAVD 88) was recorded on August 28, 2017;
10. Willow Creek near Tomball, Tex. (USGS 08068325): A peak stage of 133.87 ft above streamgage datum (water-surface elevation of 133.87 ft above NAVD 88) was recorded on August 28, 2017;
11. Bear Branch at Research Boulevard, The Woodlands, Tex. (USGS 08068390): A peak stage of 140.27 ft above streamgage datum (water-surface elevation of 140.27 ft above NAVD 88) was recorded on August 28, 2017;
12. Panther Branch at Gosling Road, The Woodlands, Tex. (USGS 08068400): A peak stage of 137.49 ft above streamgage datum (water-surface elevation of 137.49 ft above NAVD 88) was recorded on August 28, 2017;
13. Panther Branch near Spring, Tex. (USGS 08068450): A peak stage of 117.12 ft above streamgage datum (water-surface elevation of 117.12 ft above NAVD 88) was recorded on August 28, 2017;
14. Spring Creek near Spring, Tex. (USGS 08068500): A peak stage of 111.52 ft above streamgage datum (water-surface elevation of 111.56 ft above NGVD 29) was recorded on August 28, 2017;
15. West Fork San Jacinto River below Lake Conroe near Conroe, Tex. (USGS 08067650): A peak stage of 46.12 ft above streamgage datum (water-surface elevation of 162.18 ft above NGVD 29) was recorded on August 28, 2017;
16. Lake Creek at Sendera Ranch Road near Conroe, Tex. (USGS 08067920): A peak stage of 150.99 ft above streamgage datum (water-surface elevation of 150.99 ft above NAVD 88) was recorded on August 28, 2017;

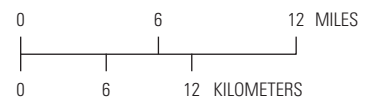
34 Characterization of Peak Streamflows and Flood Inundations from Hurricane Harvey, 2017

17. West Fork San Jacinto River near Conroe, Tex. (USGS 08068000): A peak stage of 126.93 ft above streamgage datum (water-surface elevation of 126.93 ft above NAVD 88) was recorded on August 29, 2017;
18. West Fork San Jacinto River above Lake Houston near Porter, Tex. (USGS 08068090): A peak stage of 94.87 ft above streamgage datum (water-surface elevation of 94.87 ft above NAVD 88) was recorded on August 29, 2017;
19. Caney Creek near Splendora, Tex. (USGS 08070500): A peak stage of 26.63 ft above streamgage datum (water-surface elevation of 145.07 ft above NGVD 29) was recorded on August 28, 2017;
20. Peach Creek at Splendora, Tex. (USGS 08071000): A peak stage of 25.77 ft above streamgage datum (water-surface elevation of 107.38 ft above NGVD 29) was recorded on August 28, 2017;
21. East Fork San Jacinto River near New Caney, Tex. (USGS 08070200): A peak stage of 81.15 ft above streamgage datum (water-surface elevation of 81.15 ft above NAVD 88) was recorded on August 29, 2017; and
22. Luce Bayou above Lake Houston near Huffman, Tex. (USGS 08071280): A peak stage of 37.86 ft above streamgage datum (water-surface elevation of 77.77 ft above NGVD 29) was recorded on August 29, 2017.

Rainfall totals ranged from about 17 to 43 in. within the San Jacinto Basin over the duration of the event. The highest rainfall totals from this one storm event in the San Jacinto Basin approximated the average annual rainfall for the area of about 45 in. (NOAA, 2014).



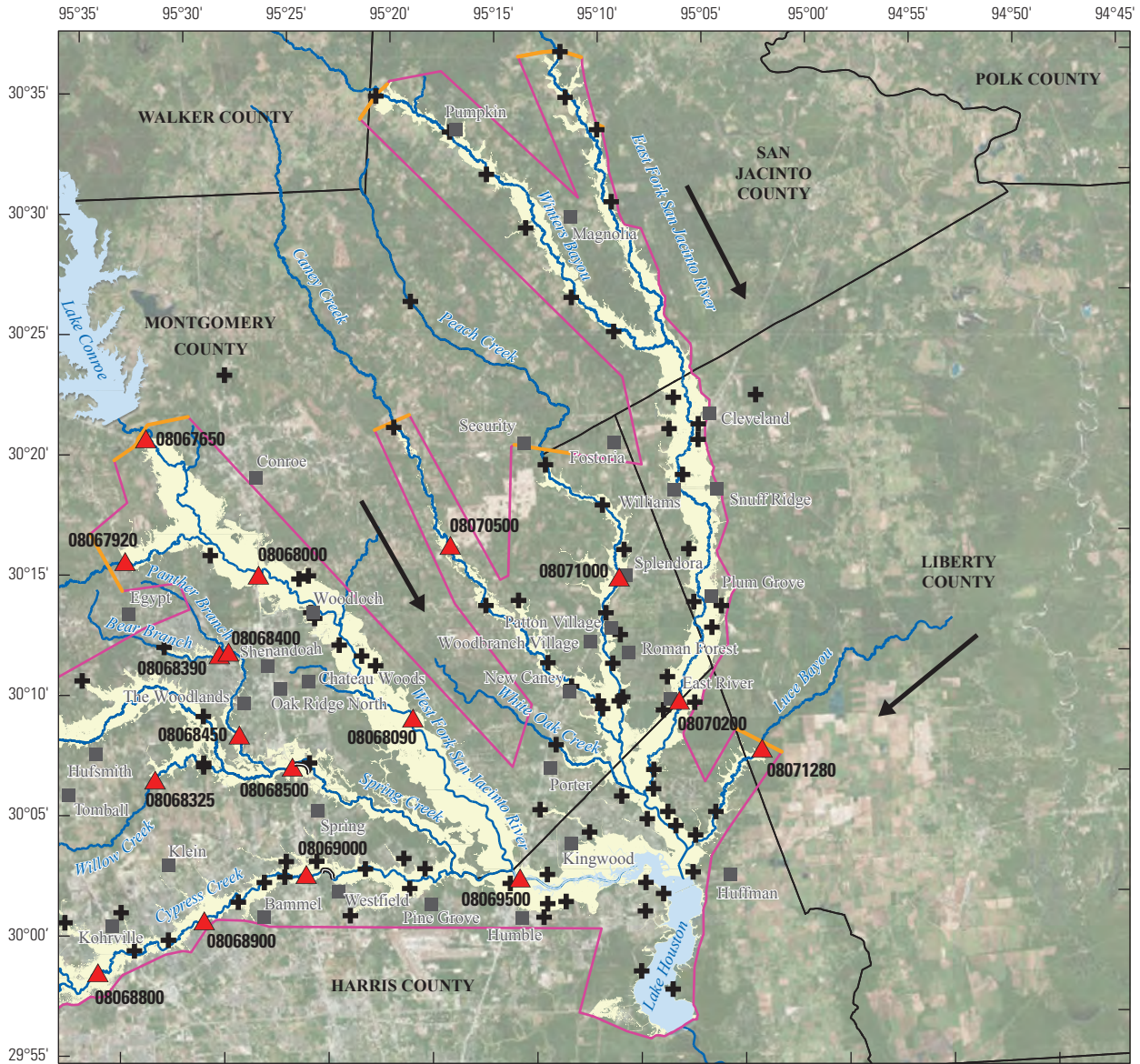
Base modified from U.S. Geological Survey digital data
 Hydrography and inundated area 1:24,000 scale
 Imagery from: Esri World Image Service
 Albers Equal Area Projection, Texas Centric Mapping System
 North American Datum of 1983 (2011)



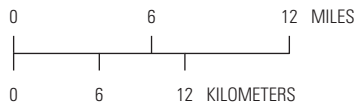
EXPLANATION

- Inundated area, derived from high-water mark water-surface elevation and streamflow-gaging station data
- Mapped boundary
- Flow direction
- Mapped area boundary—Restricted by high-water mark coverage
- Levee
- + High-water mark
- ▲ U.S. Geological Survey streamflow-gaging station and number
08067650

Figure 17. Flood-inundation map of the West Fork San Jacinto River and its tributaries for the August and September 2017 Hurricane Harvey-related flood event in southeastern Texas and southwestern Louisiana.



Base modified from U.S. Geological Survey digital data
 Hydrography and inundated area 1:24,000 scale
 Imagery from: Esri World Image Service
 Albers Equal Area Projection, Texas Centric Mapping System
 North American Datum of 1983 (2011)



EXPLANATION

- Inundated area, derived from high-water mark water-surface elevation and streamflow-gaging station data
- Mapped boundary
- Flow direction
- Mapped area boundary—Restricted by high-water mark coverage
- Levee
- + High-water mark
- ▲ U.S. Geological Survey streamflow-gaging station and number
08067650

Figure 18. Flood-inundation map of the East Fork San Jacinto River and its tributaries for the August and September 2017 Hurricane Harvey-related flood event in southeastern Texas and southwestern Louisiana.

Coastal Basins

Harvey made landfall on the northern end of San Jose Island about 5 mi east of Rockport, Tex. (fig. 1). The coastal watershed basins primarily affected by the flooding that were included in this study consist of East and West Matagorda Bay Subbasins, East and West San Antonio Bay Subbasins, and Aransas Bay Subbasin, all of which are along the southeastern coast of Texas (fig. 3; figs. 19–22). Texas coastal areas affected by Harvey begin at Matagorda Bay near the San Bernard National Wildlife Refuge south of Freeport, Tex., continue along the coast through the communities of Matagorda, Palacios near Tres Palacios Bay, Port O'Connor, Port Lavaca, Austwell, and Rockport, and continue on to the northern side of Corpus Christi Bay at Port Aransas and San Jose Island (fig. 22). The coastal basins in Texas that were affected by Harvey contain parts of Matagorda, Jackson, Calhoun, Victoria, Refugio, San Patricio, and Aransas Counties.

A total of 129 surveyed HWMs within the selected coastal basins in Texas were used to create flood-inundation maps (figs. 19–22). Peak stage elevation was recorded at the HWMs along stream reaches for the following seven streams: Peyton Creek, Big Boggy Creek, Little Boggy Creek, Tres Palacios River, East and West Carancahua Creeks, and Keller Creek. Peak stage elevation was also measured along the Texas coast. Flood-inundation maps were created for the seven stream reaches (figs. 19–21) following the same mapping methods as described previously for the watershed basins.

The USGS operates seven streamflow-gaging stations within the coastal basins that provided data used to help make the inundation maps. Data from the following streamflow-gaging stations were used:

1. Colorado River near Bay City, Tex. (USGS 08162500): A peak stage of 46.16 ft above streamgage datum (water-surface elevation of 46.16 ft above NGVD 29) was recorded on September 2, 2017;
2. Colorado River near Wadsworth, Tex. (USGS 08162501): A peak stage of 19.65 ft above streamgage datum (water-surface elevation of 26.65 ft above NAVD 88) was recorded on September 2, 2017 (provisional data);
3. Tres Palacios River near Midfield, Tex. (USGS 08162600): A peak stage of 30.21 ft above streamgage datum (water-surface elevation of 35.59 ft above NGVD 29) was recorded on August 29, 2017;
4. Garcitas Creek near Inez, Tex. (USGS 08164600): A peak stage of 24.74 ft above streamgage datum (water-surface elevation of 53.90 ft above NGVD 29) was recorded on August 27, 2017;
5. Placedo Creek near Placedo, Tex. (USGS 08164800): A peak stage of 29.77 ft above streamgage datum (water-

surface elevation of 35.35 ft above NGVD 29) was recorded on August 26, 2017;

6. Guadalupe River near Tivoli, Tex. (USGS 08188800): A peak stage of 11.78 ft above streamgage datum (water-surface elevation of 11.82 ft above NGVD 29) was recorded on September 1, 2017; and
7. Copano Creek near Refugio, Tex. (USGS 08189200): A peak stage of 16.84 ft above streamgage datum (water-surface elevation of 34.09 ft above NGVD 29) was recorded on August 29, 2017.

During the 8-day event, rainfall totals ranged from about 6.67 to 12.54 in. within the West Matagorda Bay Subbasin. Within the East Matagorda Bay Subbasin, the rainfall totals ranged from about 6.85 to 31.50 in. Within the West San Antonio Bay Subbasin, the rainfall totals ranged from about 12.02 to 17.45 in. Within the East San Antonio Bay Subbasin, the rainfall totals ranged from about 7.96 to 16.38 in., and within the Aransas Bay Subbasin, the rainfall totals ranged from about 11.65 to 33.09 in. (Blake and Zelinsky, 2018). By comparison, the mean annual precipitation for the area is about 45 in. (NOAA, 2014).

East Matagorda Bay Subbasin

Flood-inundation maps were created for several streams in the East Matagorda Bay Subbasin in Matagorda County. The flood-inundation maps cover a 17-mi reach of Peyton Creek, a 16-mi reach of Big Boggy Creek, and a 6-mi reach of Little Boggy Creek (fig. 19). A total of 11 surveyed HWMs within these reaches were used to create the inundation maps; 2 HWMs were used for the Little Boggy Creek reach, and 9 HWMs were used for the Peyton Creek and Big Boggy Creek reaches. The measured depths of water at the HWMs ranged from 0 to 3.2 ft above ground, and the water-surface elevations ranged from 3.3 to 50.7 ft above NAVD 88.

Ten surveyed HWMs were used to create a flood-inundation map for a 21-mi reach of the Tres Palacios River within Matagorda County (fig. 20). The measured depths of water at the HWMs ranged from 0 to 5.7 ft above ground, and the water-surface elevations ranged from 4.9 to 32.8 ft above NAVD 88.

Flood-inundation maps for a 13.5-mi reach of West Carancahua Creek, a 14.5-mi reach of East Carancahua Creek, and a 9.6-mi reach of Keller Creek within Matagorda, Jackson, and Calhoun Counties were created (fig. 21). A total of 11 surveyed HWMs were used to create the inundation maps for these reaches; 7 HWMs were used for the East and West Carancahua Creeks, and 4 HWMs were used for Keller Creek. The measured depths of water at the HWMs ranged from 0 to 7.7 ft above ground, and the water-surface elevations ranged from 6.7 to 21.7 ft above NAVD 88.

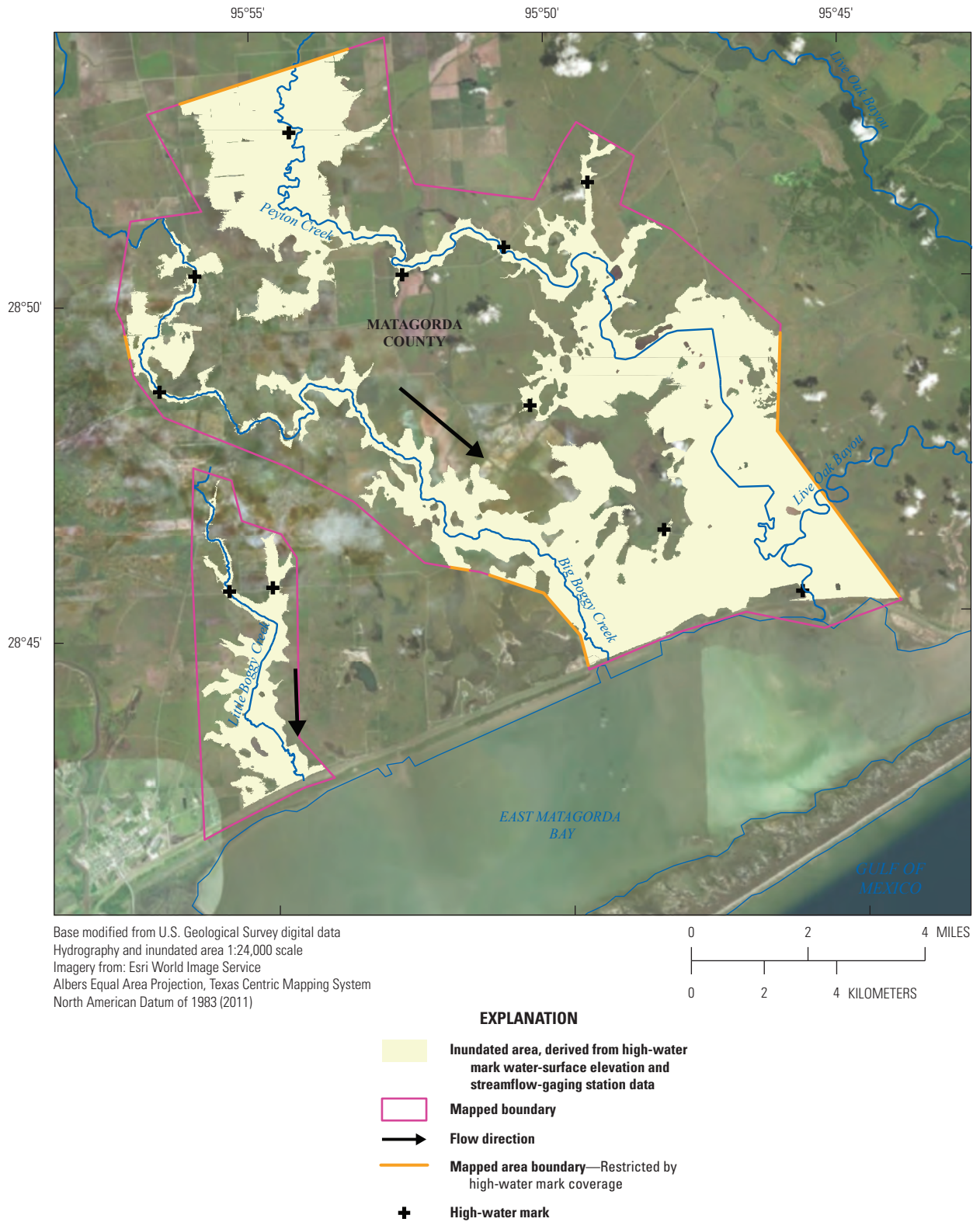
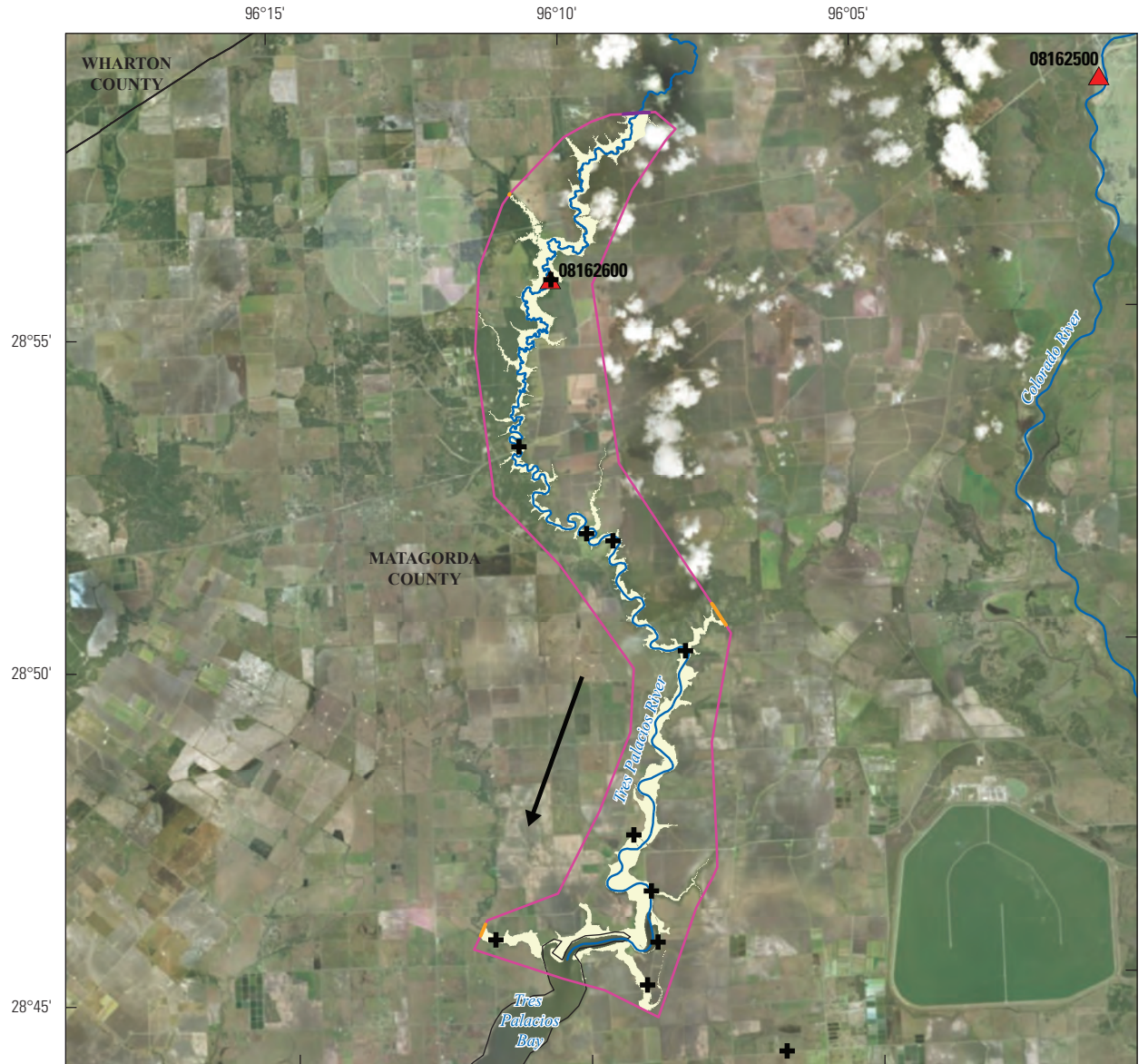


Figure 19. Flood-inundation map of Peyton Creek, Big Boggy Creek, and Little Boggy Creek for the August and September 2017 Hurricane Harvey-related flood event in southeastern Texas and southwestern Louisiana.

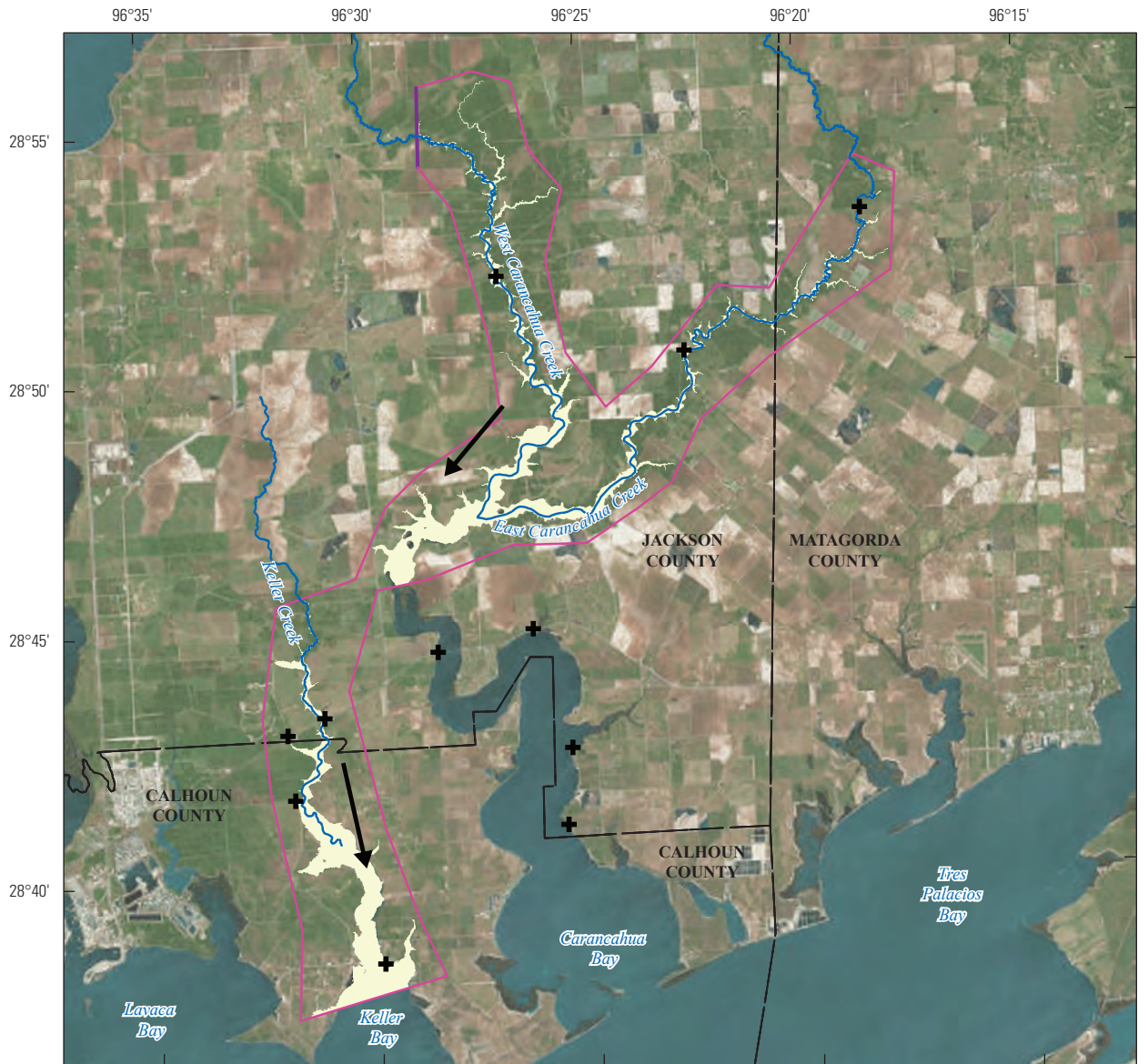


Base modified from U.S. Geological Survey digital data
 Hydrography and inundated area 1:24,000 scale
 Imagery from: Esri World Image Service
 Albers Equal Area Projection, Texas Centric Mapping System
 North American Datum of 1983 (2011)

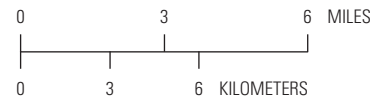


- EXPLANATION**
- Inundated area, derived from high-water mark water-surface elevation and streamflow-gaging station data
 - Mapped boundary
 - Flow direction
 - Mapped area boundary—Restricted by high-water mark coverage
 - Mapped area boundary—Restricted by lack of ground surface elevation data
 - + High-water mark
 - ▲ U.S. Geological Survey streamflow-gaging station and number

Figure 20. Flood-inundation map of the Tres Palacios River for the August and September 2017 Hurricane Harvey-related flood event in southeastern Texas and southwestern Louisiana.



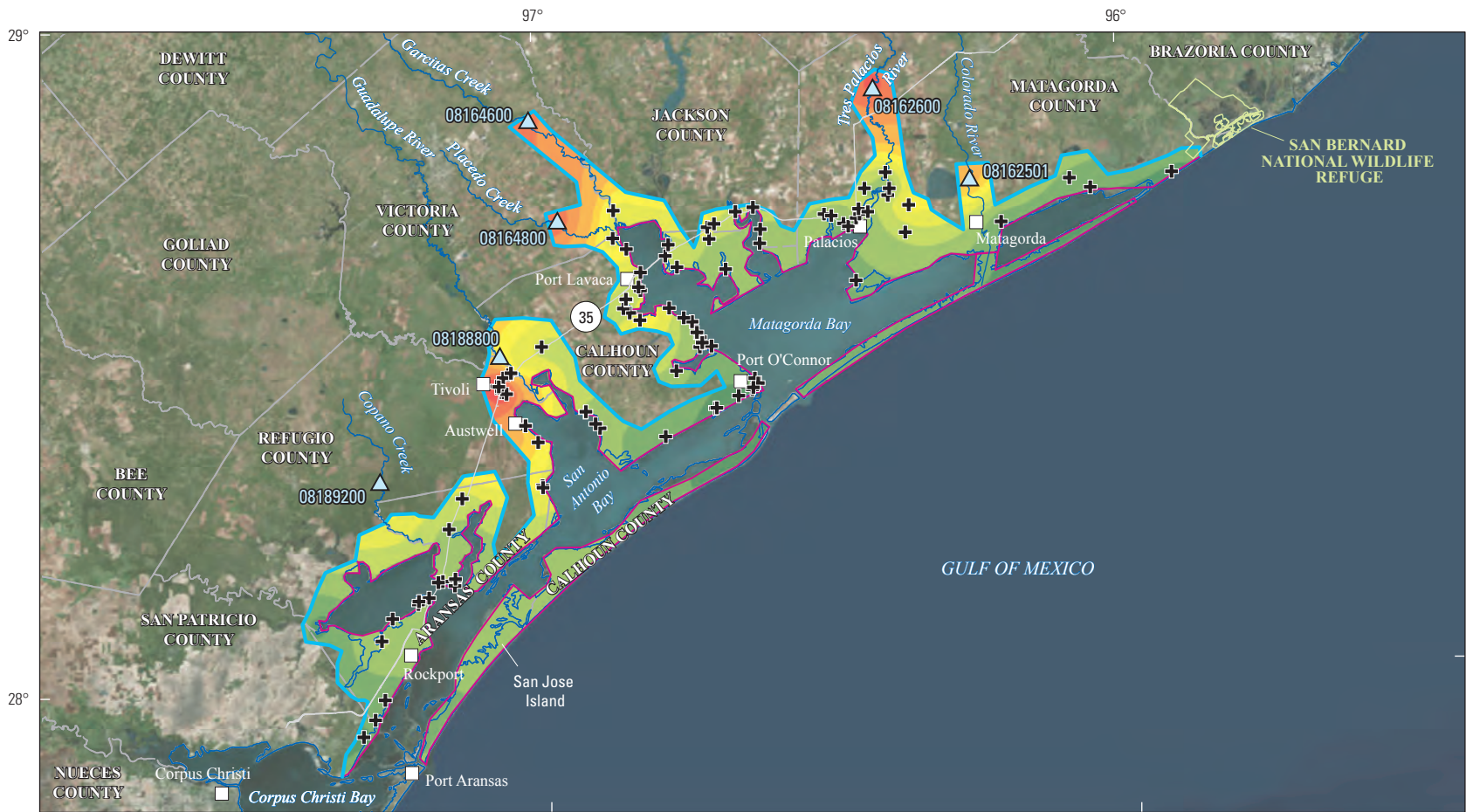
Base modified from U.S. Geological Survey digital data
 Hydrography and inundated area 1:24,000 scale
 Imagery from: Esri World Image Service
 Albers Equal Area Projection, Texas Centric Mapping System
 North American Datum of 1983 (2011)



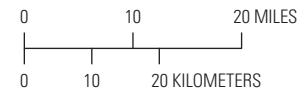
EXPLANATION

- Inundated area, derived from high-water mark water-surface elevation and streamflow-gaging station data
- Mapped boundary
- Flow direction
- Mapped area boundary—Restricted by lack of ground surface elevation data
- High-water mark

Figure 21. Flood-inundation map of the East and West Carancahua Creeks and the Keller Creek for the August and September 2017 Hurricane Harvey-related flood event in southeastern Texas and southwestern Louisiana.



Base modified from U.S. Geological Survey digital data
 Hydrography and water-surface elevation 1:24,000 scale
 Imagery from: Esri World Image Service
 Albers Equal Area Projection, Texas Centric Mapping System
 North American Datum of 1983 (2011)



EXPLANATION

Flood peaks —Water-surface elevation, in feet. Datum is North American Vertical Datum of 1988			Mapped boundary
0 to 2	8.1 to 10	16.1 to 20	Mapped area boundary —Restricted by high-water mark coverage
2.1 to 4	10.1 to 12	20.1 to 24	High-water mark
4.1 to 6	12.1 to 14	24.1 to 28	U.S. Geological Survey streamflow-gaging station and number
6.1 to 8	14.1 to 16	28.1 to 34.4	

Figure 22. Flood-inundation map from coastal water-surface elevation data for the August and September 2017 Hurricane Harvey-related flood event in southeastern Texas and southwestern Louisiana.

Peak Water-Surface Elevations for Coastal Areas

The coastal water-surface elevation map for the 135-mi coastline of Texas including the counties of Matagorda, Jackson, Calhoun, Victoria, Refugio, San Patricio, and Aransas is shown in figure 22. A total of 97 surveyed HWMs and 6 USGS streamflow-gaging stations were used to create the coastal water-surface elevation map. This map shows the water-surface elevation, generated from topo to raster interpolation methods, from peak stage recorded during the flood event. The mapped boundary was kept in close proximity to the location of surveyed HWMs. The measured depths of water at the HWMs ranged from 0 to 4.8 ft above ground, and the water-surface elevations ranged from 2.7 ft above NAVD 88 near Port O'Connor to 34.4 ft above NAVD 88 along State Highway 35 near Tivoli.

Flood Damages

More than 300,000 structures and at least 500,000 cars were flooded as a result of Harvey (NOAA, 2018c). The most current (2018) damage estimate from Harvey is \$125 billion, making it the second costliest event behind Hurricane Katrina in 2005 when adjusted for inflation (NOAA, 2018c). Harvey ranks as the deadliest hurricane to hit the United States since Hurricane Sandy in 2012. Harvey is responsible for at least 68 direct fatalities, all in Texas. Direct fatalities are those that are a direct result of the tropical storm such as lightning, wind-related collapses, and drowning from storm surge, rough seas, rip currents, and freshwater flooding. All but three of the fatalities were a result of freshwater flooding; none of the fatalities resulted from storm surge. In addition to the 68 direct fatalities, an additional 35 people died as a result of indirect causes such as electrocution, vehicle crashes, and lack of medical services (NOAA, 2018c).

Summary

Hurricane Harvey made landfall near Rockport, Texas, on August 25 as a Category 4 hurricane with wind gusts exceeding 150 miles per hour. As Harvey moved inland, the forward motion of the storm slowed down and produced tremendous rainfall amounts to southeastern Texas, with 8-day rainfall amounts exceeding 60 inches in some locations, which is about 15 inches more than average annual amounts of rainfall for eastern Texas and the Texas coast. Historic flooding occurred in Texas as a result of the widespread, heavy rainfall.

In the immediate aftermath of the Harvey-related flood event, the U.S. Geological Survey (USGS) and the Federal Emergency Management Agency (FEMA) initiated a cooperative study to evaluate the magnitude of the flood, determine the probability of occurrence, and map the extent

of the flood in Texas. Seventy-four USGS streamflow-gaging stations in Texas with at least 15 years of record and no large data gaps in the period of record had a 2017 annual peak streamflow related to Harvey ranking in the top five of all annual peaks for each given station. New record peak streamflows were recorded at 40 of the 74 USGS streamflow-gaging stations. The number of years of peak streamflow record for the 74 analyzed streamflow-gaging stations ranged from 18 to 105, with a mean of 55 years. The annual exceedance probability estimates for the analyzed streamflow-gaging stations ranged from less than 0.2 to 14.0 percent. During the weeks following the event, USGS field crews surveyed 2,123 high-water marks to obtain water-surface elevations. In some locations, several water-surface elevations were averaged to obtain 1 water-surface elevation, resulting in 1,258 water-surface elevations. Some of these high-water marks were used, along with peak-stage data from USGS streamflow-gaging stations, to create 19 inundation maps of the extent of the maximum depth of the flooding.

References Cited

- Benson, M.A., and Dalrymple, Tate, 1967, General field and office procedures for indirect measurements: U.S. Geological Survey Techniques of Water-Resources Investigations, book 3, chap. A1, 30 p. [Also available at <http://pubs.er.usgs.gov/publication/twri03A1>.]
- Blake, E.S., and Zelinsky, D.A., 2018, Hurricane Harvey, National Oceanic and Atmospheric Administration, National Hurricane Center Tropical Cyclone Report, 76 p., accessed February 26, 2018, at https://www.nhc.noaa.gov/data/tcr/AL092017_Harvey.pdf.
- Cohn, T.A., Lane, W.L., and Baier, W.G., 1997, An algorithm for computing moments-based flood quantile estimates when historical flood information is available: Water Resources Research, v. 33, no. 9, p. 2089–2096.
- Cohn, T.A., Lane, W.L., and Stedinger, J.R., 2001, Confidence intervals for Expected Moments Algorithm flood quantile estimates: Water Resources Research, v. 37, no. 6, p. 1695–1706.
- England, J.F., Jr., Cohn, T.A., Faber, B.A., Stedinger, J.R., Thomas, W.O., Jr., Veilleux, A.G., Kiang, J.E., and Mason, R.R., Jr., 2018, Guidelines for determining flood flow frequency—Bulletin 17C: U.S. Geological Survey Techniques and Methods, book 4, chap. B5, 148 p., accessed April 2, 2018, at <https://doi.org/10.3133/tm4B5>.
- Fenneman, N.M., 1946, Physical divisions of the United States: U.S. Geological Survey map, scale 1:7,000,000, 1 sheet.

- Flynn, K.M., Kirby, W.H., and Hummel, P.R., 2006, User's manual for program PeakFQ annual flood-frequency analysis using Bulletin 17B guidelines: U.S. Geological Survey Techniques and Methods, book 4, chap. B4, 42 p. [Also available at <https://www.nrc.gov/docs/ML0933/ML093340269.pdf>.]
- Grubbs, F., and Beck, G., 1972, Extension of sample sizes and percentage points for significance tests of outlying observations: *Technometrics*, v. 14, no. 4, p. 847–854.
- Holmes, R.R., Jr., and Dinicola, Karen, 2010, 100-Year flood—It's all about chance: U.S. Geological Survey General Information Product 106, 1 p. [Also available at <https://pubs.usgs.gov/gip/106/>.]
- Interagency Advisory Committee on Water Data [IACWD], 1982, Guidelines for determining flood flow frequency: Reston, Va., U.S. Geological Survey, Office of Water Data Coordination, Hydrology Subcommittee Bulletin 17B [variously paged].
- Judd, L.J., Asquith, W.H., and Slade, R.M., Jr., 1996, Techniques to estimate generalized skew coefficients of annual peak streamflow for natural basins in Texas: U.S. Geological Survey Water-Resources Investigations Report 96–4117, 28 p. [Also available at <https://pubs.usgs.gov/wri/wri964117/>.]
- Koenig, T.A., Bruce, J.L., O'Connor, J.E., McGee, B.D., Holmes, R.R., Jr., Hollins, Ryan, Forbes, B.T., Kohn, M.S., Schellekens, M.F., Martin, Z.W., and Pepler, M.C., 2016, Identifying and preserving high-water mark data: U.S. Geological Survey Techniques and Methods, book 3, chap. A24, 47 p. [Also available at <http://dx.doi.org/10.3133/tm3A24>.]
- Mason, R.R., Jr., 2012, Office of Surface Water Technical Memorandum No. 2013.01, Computation of annual exceedance probability (AEP) for characterization of observed flood peaks, accessed March 6, 2018, at <https://water.usgs.gov/admin/memo/SW/sw13.01.pdf>.
- Musser, J.W., Watson, K.M., Painter, J.A., and Gotvald, A.J., 2016, Flood-inundation maps of selected areas affected by the flood of October 2015 in central and coastal South Carolina: U.S. Geological Survey Open-File Report 2016–1019, 81 p., accessed March 2018 at <http://dx.doi.org/10.3133/ofr20161019>.
- National Oceanic and Atmospheric Administration [NOAA], 2014, NCDC climate data online, retrieval menu, accessed November 25, 2014, at <http://www7.ncdc.noaa.gov/CDO/CDODivisionalSelect.jsp#>.
- National Oceanic and Atmospheric Administration [NOAA], 2017, U.S. climatological divisions, accessed February 9, 2017, at <https://www.ncdc.noaa.gov/monitoring-references/maps/images/us-climate-divisions-names.jpg>.
- National Oceanic and Atmospheric Administration [NOAA], 2018a, Hurricane Harvey info, accessed February 15, 2018, at <http://www.weather.gov/hgx/hurricaneharvey>.
- National Oceanic and Atmospheric Administration [NOAA], 2018b, Major Hurricane Harvey – August 25–29, 2017, accessed February 15, 2018, at http://www.weather.gov/crp/hurricane_harvey.
- National Oceanic and Atmospheric Administration [NOAA], 2018c, Billion-dollar weather and climate disasters: Table of events, accessed February 15, 2018, at <http://www.ncdc.noaa.gov/billions/events>.
- Rantz, S.E., and others, 1982a, Measurement and computation of streamflow: Volume 1. Measurement of stage and discharge: U.S. Geological Survey Water-Supply Paper 2175, v. 1, p. 1–284. [Also available at http://pubs.usgs.gov/wsp/wsp2175/pdf/WSP2175_vol1a.pdf.]
- Rantz, S.E., and others, 1982b, Measurement and computation of streamflow: Volume 2. Computation of discharge: U.S. Geological Survey Water-Supply Paper 2175, v. 2, p. 285–631. [Also available at http://pubs.usgs.gov/wsp/wsp2175/pdf/WSP2175_vol2a.pdf.]
- Texas A&M Forest Service, 2018, Texas Ecoregions, accessed March 28, 2018, at <http://texastreeid.tamu.edu/content/texasEcoRegions/Pineywoods/>.
- Texas Natural Resources Information System, 2006, FEMA 2006 140cm Lidar: Federal Emergency Management Agency, accessed December 5, 2017, at <https://tnris.org/data-catalog/entry/fema-2006-140cm/>.
- Texas Natural Resources Information System, 2007, CAPCOG 2008 140cm Lidar: Capital Area Council of Governments, accessed December 5, 2017, at <https://tnris.org/data-catalog/entry/capcog-2008-140cm/>.
- Texas Natural Resources Information System, 2008, Houston-Galveston Area Council (H-GAC) 2008 Lidar: Houston-Galveston Area Council and Merrick & Company, accessed December 5, 2017, at <https://tnris.org/data-catalog/entry/houston-galveston-area-council-h-gac-2008-lidar/>.
- Texas Natural Resources Information System, 2009 StratMap 2009 1m Goliad, McMullen, Zapata Lidar: Texas Natural Resources Information System, accessed December 5, 2017, at <https://tnris.org/data-catalog/entry/stratmap-2009-1m-goliad-mcmullen-zapata/>.
- Texas Natural Resources Information System, 2010, StratMap 2010 1m Lee, Leon, Madison & Milam Lidar: Texas Natural Resources Information System, accessed December 5, 2017, at <https://tnris.org/data-catalog/entry/stratmap-2010-1m-lee-leon-madison-milam/>.

- Texas Natural Resources Information System, 2011a, FEMA 2011 1m Liberty Lidar: Federal Emergency Management Agency, accessed December 5, 2017, at <https://tnris.org/data-catalog/entry/fema-2011-1m-liberty/>.
- Texas Natural Resources Information System, 2011b, StratMap 2011 50cm Austin, Grimes, Walker Lidar: Texas Natural Resources Information System, accessed December 5, 2017, at <https://tnris.org/data-catalog/entry/stratmap-2011-50cm-austin-grimes-walker/>.
- Texas Natural Resources Information System, 2011c, StratMap 2011 1M Shelby, Sabine and Newton Lidar: Texas Natural Resources Information System, accessed December 5, 2017, at <https://tnris.org/data-catalog/entry/stratmap-2011-1m-shelby-sabine-and-newton/>.
- Texas Natural Resources Information System, 2011d, USGS 2011 150cm Lidar: U.S. Geological Survey, accessed December 5, 2017, at <https://tnris.org/data-catalog/entry/usgs-2011-150cm/>.
- Texas Natural Resources Information System, 2012, StratMap 2012 50cm TCEQ Dam Safety Sites Lidar: Texas Natural Resources Information System, accessed December 5, 2017, at <https://tnris.org/data-catalog/entry/stratmap-2012-50cm-tceq-dam-safety-sites/>.
- Texas Natural Resources Information System, 2013, StratMap 2013 50cm Ellis, Navarro, Wilson & Karnes Lidar: Texas Natural Resources Information System, accessed December 5, 2017, at <https://tnris.org/data-catalog/entry/stratmap-2013-50cm-ellis-navarro-wilson-karnes/>.
- Texas Natural Resources Information System, 2014, StratMap 2014 50cm Fort Bend Lidar: Texas Natural Resources Information System, accessed December 5, 2017, at <https://tnris.org/data-catalog/entry/stratmap-2014-50cm-fort-bend/>.
- Texas Natural Resources Information System, 2016, FEMA 2016 DeWitt County Lidar: Federal Emergency Management Agency, accessed December 5, 2017, at <https://tnris.org/data-catalog/entry/fema-2016-dewitt/>.
- Texas Natural Resources Information System, 2017, StratMap 2017 50cm East Texas Lidar: Texas Natural Resources Information System, accessed December 5, 2017, at <https://tnris.org/data-catalog/entry/stratMap-2017-50cm-east-texas-lidar/>.
- Texas State Historical Association, 2018, Physical Regions of Texas, accessed February 22, 2018, at <https://texasalmanac.com/topics/environment/physical-regions-texas>.
- Turnipseed, D.P., and Sauer, V.B., 2010, Discharge measurements at gaging stations: U.S. Geological Survey Techniques and Methods, book 3, chap. A8, 87 p. [Also available at <http://pubs.usgs.gov/tm/tm3-a8/>.]
- U.S. Geological Survey [USGS], 2018a, USGS surface-water data for the Nation, *in* USGS water data for the Nation: U.S. Geological Survey National Water Information System database, accessed February 13, 2018, at <https://doi.org/10.5066/F7P55KJN>. [Surface-water information directly accessible at <https://waterdata.usgs.gov/nwis/sw/>.]
- U.S. Geological Survey [USGS], 2018b, Short-Term Network Data Portal: USGS flood information web page, accessed February 13, 2018, at <https://water.usgs.gov/floods/FEV>.
- U.S. Geological Survey [USGS], 2018c, Special Topic—Hurricane Harvey: USGS flood information, accessed February 13, 2018, at <https://www.usgs.gov/special-topic/hurricane-harvey>.
- U.S. Geological Survey [USGS], 2018d, PeakFQ, flood frequency analysis based on Bulletin 17B and recommendations of the Advisory Committee on Water Information (ACWI) Subcommittee on Hydrology (SOH) Hydrologic Frequency Analysis Work Group (HFAWG), accessed February 10, 2018, at <https://water.usgs.gov/software/PeakFQ/>.
- U.S. Geological Survey [USGS], The National Map, 2018, 3DEP products and services: The National Map, 3D Elevation Program web page, accessed May 2018 at https://nationalmap.gov/3DEP/3dep_prodserv.html.
- Veilleux, A.G., Cohn, T.A., Flynn, K.M., Mason, R.R., Jr., and Hummel, P.R., 2014, Estimating magnitude and frequency of floods using the PeakFQ 7.0 program: U.S. Geological Survey Fact Sheet 2013–3108, 2 p., accessed March 2018 at <https://doi.org/10.3133/fs20133108>.
- Watson, K.M., Storm, J.B., Breaker, B.K., and Rose, C.E., 2017, Characterization of peak streamflows and flood inundation of selected areas in Louisiana from the August 2016 flood: U.S. Geological Survey Scientific Investigations Report 2017–5005, 26 p., accessed March 2018 at <https://pubs.er.usgs.gov/publication/sir20175005>.
- Watson, K.M., Welborn, T.L., Stengel, V.G., Wallace, D.S., and McDowell, J.S., 2018, Data used to characterize peak streamflows and flood inundation resulting from Hurricane Harvey of selected areas in southeastern Texas and southwestern Louisiana, August–September 2017: U.S. Geological Survey data release, <https://doi.org/10.5066/F7VH5N3N>.

For more information about this publication, contact

Director, Texas Water Science Center
U.S. Geological Survey
1505 Ferguson Lane
Austin, TX 78754-4501

For additional information visit <https://tx.usgs.gov/>.

Publishing support provided by
Lafayette Publishing Service Center

